Viscous Evolution of Black Hole Accretion Disks

A Thesis

submitted to
Indian Institute of Science Education and Research Pune
in partial fulfillment of the requirements for the
BS-MS Dual Degree Programme

by

Prashali Chauhan
Reg. no. 20121094

IISER PUNE

Indian Institute of Science Education and Research Pune
Dr. Homi Bhabha Road,
Pashan, Pune 411008, INDIA.

May, 2017

Supervisor: **Dr. Prasad Subramanian**
© **Prashali Chauhan** 2017

All rights reserved

Certificate

This is to certify that this dissertation entitled Viscous Evolution of Black Hole Accretion Diskstowards the partial fulfilment of the BS-MS dual degree programme at the Indian Institute of Science Education and Research, Pune represents study/work carried out by **Prashali Chauhan** at Indian Institute of Science Education and Research under the supervision of **Dr. Prasad Subramanian**, Associate Professor, Department of Physics, during the academic year 2016-2017.

Dr. Prasad Subramanian

Committee:

Dr. Prasad Subramanian

Dr. Apratim Chatterjee

In the memory of my Grandmother.

Declaration

I hereby declare that the matter embodied in the report entitled Viscous Evolution of Black Hole Accretion Disks are the results of the work carried out by me at the Department of Physics, Indian Institute of Science Education and Research, Pune under the supervision of **Dr. Prasad Subramanian** and the same has not been submitted elsewhere for any other degree.

Prashali
28th Mar' 17

Prashali Chauhan

Acknowledgments

I would like to express gratitude to my parents for their continuous support and faith in me. They have always stood by my choices and decisions. I would like to thank my supervisor, Dr. Prasad Subramanian for guiding me through the past 2 years. I am also thankful to all my friends here at IISER for making it a memorable 5 years.

Lastly, I would also like to acknowledge INSPIRE, DST for the continuous financial support and Government of India for their support for basic sciences.

Abstract

Accretion disks around black holes are at the heart of much of the activity observed in active galactic nuclei and galactic microquasars. In turn, the structure of accretion disks is governed by the micro-physical viscosity mechanism that enables nearby plasma to lose its angular momentum and go accrete onto the black hole.

In this work, we focus on hot, two-temperature accretion disks where the ions are collisionless. We study two possible viscosity mechanisms. In the first model, we assume a random magnetic field present throughout the disk and characterize it using the ion inertial length as magnetic coherence length. In the second model, we use radial diffusion of ions across the large-scale toroidal magnetic field to characterize the coefficient of viscosity.

Systems with an accretion disk also often harbor powerful jets that are often episodic. We attempt to understand the disk-jet connection using the second model to interpret observations of X-ray variations from active radio galaxy 3C 120. We compare the time scale of the observed variations to the viscous time scale associated with this particular disk model. We envisage a viscous instability which results in disk collapse and possible episodic ejections of blobs. Our work represents the first attempt to quantify this scenario with a specific viscosity model.

Contents

Abstract **xi**

1 Introduction **3**

1.1 Two Temperature Disk 4

2 ION VISCOSITY BASED ON ION INERTIAL LENGTH **7**

2.1 Hybrid Viscosity 8

2.2 Two Temperature Accretion Disk Model 10

2.3 Results and inferences 12

3 VISCOSITY DUE TO DIFFUSION OF CHARGED PARTICLES THROUGH MAGNETIC FIELDS **17**

3.1 Transport coefficients 18

3.2 Hybrid Viscosity 18

3.3 Two-Temperature Accretion Disk Model 19

3.4 Results 20

4 Instability of Disk and Viscous timescales **27**

4.1 Disk Instability 27

4.2 Viscous Timescales and Comparison with Observations 30

5 Results and Discussion 37

5.1 Summary 37

5.2 Further work 38

List of Figures

2.1 α for different accretion rates 13

2.2 τ_{es} for different accretion rates 14

2.3 ξ for different accretion rates 14

2.4 N_i for different accretion rates 15

3.1 T_i for Kolmogorov process for accretion rates of 0.0001, 0.0005, and 0.001. . 21

3.2 α for Kolmogorov process for the given accretion rates of 0.0001, 0.0005, and 0.001. 22

3.3 τ_{es} for Kolmogorov spectrum (Independent of accretion rate). 23

3.4 Kolmogorov Spectrum: Temperature/10^{13} for different accretion rates . . . 23

3.5 Kolmogorov Spectrum: $\frac{H}{R}$ (Independent of accretion rate) 24

3.6 Kraichnan Spectrum: α for different accretion rates 24

3.7 τ_{es} for Kraichnan spectrum (Independent of accretion rate). 25

3.8 Kraichnan Spectrum: Temperature/10^{13} for different accretion rates 25

3.9 Kraichnan Spectrum: $\frac{H}{R}$ (Independent of accretion rate). 26

4.1 t_{visc} for Kolmogorov process for different accretion rates 31

4.2 X-ray dip observations for 3C 120 33

4.3 $\frac{t_{visc}}{t_{max}}$ for $\frac{\dot{M}}{M_E} = 0.0001$ and 0.0005 34

4.4 $\frac{t_{visc}}{t_{min}}$ for $\frac{\dot{M}}{M_E} = 0.0001$ and 0.0005 34

4.5 $\frac{t_{visc}}{t_{avg}}$ for $\frac{\dot{M}}{M_E} = 0.0001$ and 0.0005 35

4.6 $\mathcal{M}_{\phi}$ for different accretion rates for Kolmogorov process 35

5.1 Observation of X-ray, Radio and Optical flux from 3C 120. 41

Chapter 1

Introduction

An accretion disk is a structure formed by diffused matter which gets pulled in the gravitational field of a massive compact object. The central object can be a star, or black hole, or an Active-Galactic Nuclei (AGN). In most accretion processes in the presence of magnetic field, the infalling matter has angular momentum. It can approach the center only if there is a mechanism in place to transport the angular momentum outwards. It is thought to be done via micro-physical viscosity, but the exact mechanism is not known.

Many important astrophysical systems, like AGNs, quasars, etc., possess relativistic outflows or jets. These require generation of a large amount of energy in a compact region. The nearby gas and dust act like the fuel. This gas, in most cases, has angular momentum which leads to the formation of an accretion disk around the central object. It suggests that there exists a direct link between these phenomena and accretion process. This makes the question of the mechanism of angular momentum transport, an important one.

Shakura and Sunyaev [1], in their seminal paper, suggested parameterizing viscosity using an 'α' parameter in terms of pressure. This parameter incorporates all the physical details we don't know about the viscosity.

In the following chapters we attempt to provide a model for viscosity to be able to explain the observations of emissions from AGNs in the form of relativistic jets or the X-ray spectrum. We focus on two-temperature, quasi-Keplerian accretion disks.

In the first part, we discuss a hybrid viscosity due to the presence of turbulent magnetic fields and Coulomb collisions, where the magnetic coherence length of ions is defined by the ion inertial length. We show what kind of disk this model gives rise to. In the second part, we model the viscosity coefficient based on the diffusion based transport coefficients. We present the disk model it gives rise to and compare the viscous timescale of such a disk with observations from active radio galaxy, 3C 120 [2].

1.1 Two Temperature Disk

For all the following discussions we have assumed a two-temperature disk. It was introduced by Shapiro, Lightman, and Eardley [3] to explain the spectrum of Cyg-X1 and since has been extensively used [4]. The structure of two-temperature disk is thought to be made of a bloated inner region of accretion around a black hole, surrounded by a cool thin disk. Here, I will derive the basic disk structure equations for the steady state which we will use later on to build upon the viscosity models.

Assume a quasi-keplerian disk with no vertical structure and cylindrical symmetry with accretion rate $\dot{M}$. We take H to be the half-thickness of the disk, R, radius, ρ to be mass density. The azimuthal velocity, v_ϕ will be $\sqrt{\frac{GM}{R}}$.

Hydrostatic Equilibrium:

We have assumed the disk to be in a vertical hydrostatic equilibrium so the vertical component of momentum becomes:

$$\frac{1}{\rho}\frac{\partial P}{\partial z} = \frac{\partial}{\partial z}\left(\frac{GM}{\sqrt{R^2+z^2}}\right) \tag{1.1}$$

The term inside the partial derivative gives the force on a point particle. For a thin disk,

$$\frac{1}{\rho}\frac{\partial P}{\partial z} = -\frac{GMz}{R^3}$$

$$\frac{\partial P}{\partial z} \sim -\frac{P}{H}, \; z \sim H$$

we get:

$$\boxed{P = \frac{GM\rho H^2}{R^3}} \tag{1.2}$$

Angular Momentum conservation:

That is, angular momentum of the matter being swept in due to viscous stress, is conserved at every point.

$$\text{(viscous stress).(area)}R = \text{(Angular momentum per unit mass).(accretion rate)}$$

As defined by Shakura and Sunyaev [1], viscous stress is given by αP. We get the final equation to be :

$$\alpha P\,.(2\pi RH).R = (G\,M\,R)^{1/2}\dot{M} \tag{1.3}$$

$$\Rightarrow \boxed{\alpha P = \frac{(GMR)^{1/2}\dot{M}}{4\pi R^2 H}} \tag{1.4}$$

Equation of state:

$$P = \rho k_B (T_i + T_e)/m_p \tag{1.5}$$

where, T_i is ion temperature, T_e is electron temperature, and ρ is the mass density. $\rho = N_i m_p$, with N_i being the number density of ions.

$$\boxed{P = N_i k_B (T_i + T_e)} \tag{1.6}$$

Ion Thermal Balance:

We have assumed the ions and electrons to be interacting only via Coulomb collisions. All the energy from viscous dissipation is used up in heating the ions and consequently electrons via Coulomb interactions. Energy dissipated due to viscous stress is:

$$D(R) = \frac{3}{8\pi}\frac{GM\dot{M}}{R^3} \tag{1.7}$$

With $ln\,\Lambda$ being Coulomb logarithm (ratio of maximum to minimum impact parameter for

Coulomb collisions), the ion thermal balance equation is:

$$\boxed{\frac{3}{8\pi}\frac{GM\dot{M}}{R^3H} = 3.75\times 10^{21}\, m_i\, ln\,\Lambda\, N_i^2\, k_B \frac{(T_i - T_e)}{T_e^{3/2}}} \tag{1.8}$$

Inverse Compton cooling We assume electron to cool via inverse Compton process. With y being Compton parameter, temperature of electron is given by:

$$\boxed{T_e = \frac{m_e c^2 y}{4k_B}\frac{1}{\tau_{es} g(\tau_{es})}} \tag{1.9}$$

Here, $g(\tau_{es}) = 1 + \tau_{es}$.
And finally, optical depth given as:

$$\boxed{\tau_{es} = N_i\,\sigma_T\,H} \tag{1.10}$$

with σ_T being Thomson's scattering cross section.

All the above calculations are done using classical equations, but as we go close to the black hole, general relativistic effects become significant. The above equations are considered to be valid only till $3R_g$, as after that Keplerian assumption starts to break down. To make it more general, we have added relativistic correction factors, f_1, f_2, f_3 as calculated by Eilek (1980) [5] for Kerr metric.
Equation 1.2 becomes:

$$P = \frac{G\,M\,m_i\,N_i\,H^2 f_1}{R^3} \tag{1.11}$$

Equation 1.4:

$$\alpha P = \frac{(GMR)^{1/2}\dot{M}\,f_2}{4\pi R^2 H} \tag{1.12}$$

and equation 1.8 becomes:

$$\frac{3}{8\pi}\frac{GM\dot{M}}{R^3H}f_3 = 3.75\times 10^{21}\, m_i\, ln\,\Lambda\, N_i^2\, k_B \frac{(T_i - T_e)}{T_e^{3/2}} \tag{1.13}$$

We have used the above modified equations along with equations 1.6, 1.9 and 1.10 to calculate various disk parameters for the models discussed later.

Chapter 2

ION VISCOSITY BASED ON ION INERTIAL LENGTH

The problem of transport of angular momentum across the disk is an old one. It is thought to occur via viscous mechanisms, but molecular viscosity by itself doesn't explain the accretion rates reached to be able to justify the various emissions we observe. In the initial part of the project, we were working on a viscosity model based on shear stress in the accretion disk in presence of tangled magnetic fields, largely based on the work done in Subramanian, Becker, Kafatos, 1996 [6] (referred as SBK96 from here). Ion viscosity arises from Coulombic interactions, giving mean free path for the process as Coulomb mean free path, but the disk may also have magnetic fields present which can have significant affect on viscosity. The presence of magnetic fields drastically alters the transport properties. SBK96 assume a tangled magnetic field embedded in the accretion disk. The magnetic field kinks play the part of scattering centers and the operative mean free path essentially becomes the coherence length of the tangled magnetic field. They have taken the coherence length to be a free parameter. In this work, we adopt a different approach and adopt a specific prescription for the mean free path. Sections 2.1.1 - 2.1.2 below sketch the formalism of SBK96 for completeness and section 2.2.2 - 2.2.3 outlines the concept of the ion inertial length, which we take to be the mean free path.

2.1 Hybrid Viscosity

2.1.1 Viscosity due to Coulomb collisions

Consider a field free plasma with viscosity constant, η_{ff}, and velocity profile, $u(y)\hat{z}$. The shear stress is equal to net flux of momentum in the vertical direction across radial direction. λ_{ii} is the ionic mean free path, that is, it defines the average length scale over which the exchange of momentum is taking place.

$$-\eta_{ff}\frac{du}{dy} = -N_i\sqrt{\frac{kT_i}{2\pi m_i}}m_i\frac{du}{dy}\lambda_{ii}2 \tag{2.1}$$

here, N_i is ionic density and T_i is ionic temperature. We can see that velocity of particles varies over a length scale of λ_{ii}

We assume plasma to be made up of completely ionized hydrogen, so mean free path is given by:

$$\lambda_{ii} = v_{rms}t_{ii}$$

where v_{rms} is the root mean square velocity of Maxwellian distribution and t_{ii} is the mean time between Coulomb collisions.

The interactions, in this case, take place over a characteristic length scale of λ_{ii}. But in the case of accretion, many times velocity might vary over lengths larger than the characteristic length, then the above won't be valid anymore.

We haven't considered the effect of magnetic fields present in the disk yet. If we assume a uniform magnetic field in the $\hat{z}$ direction that is perpendicular to the velocity gradient. We have one more length scale in the picture, λ_L, Larmor radius of the ions. The momentum carried by the ions will now be $(du/dy)\lambda_L m_i$, with an extra factor of (λ_L/λ_{ii}) for the probability of particle undergoing Coulomb collision before completing a full circle. The cross field viscosity now will be given by:

$$-\eta_{\perp}\frac{du}{dy} = -2N_i\sqrt{\frac{kT_i}{2\pi m_i}}m_i\frac{du}{dy}\lambda_L\frac{\lambda_L}{\lambda_{ii}} \tag{2.2}$$

2.1.2 Tangled magnetic fields

The picture above doesn't give a realistic view of the magnetic fields in accretions disk. The magnetic field might often be generated dynamically in the accretion disk, unlike the constant field we had above. For the following calculations, we assume that the fields vary randomly in time and space or is tangled. The field is assumed to be tangled in a self similar manner with coherence length to be λ_{coh}. Here unlike the previous case, the ions are not always moving perpendicularly to a fixed field. At any given instant the ions will be gyrating around randomly oriented magnetic field. We can see that only the component of momentum parallel to the magnetic field will be conserved unless the ion undergoes a Coulomb collision or hops on to a different magnetic field line.

These magnetic 'kinks' or irregularities depend on the kind of turbulence the medium has. The momentum can transfer into the gas by either of the two processes, Coulomb interaction or through magnetic irregularities. The probability of either happening is related to their respective mean free paths. If we assume them to be statistically uncorrelated, the effective mean free path can be given as:

$$\frac{1}{\lambda} = \frac{1}{\lambda_{ii}} + \frac{1}{\lambda_{coh}} \tag{2.3}$$

where λ_{coh} is the average length of magnetic kinks.

We assume same velocity distribution, of $u(y)\hat{z}$ and isothermal ions with temperature, T_i. From the frame of reference of the plasma, the ions have Maxwellian velocity distribution. We only consider the transport of momentum along the field lines. Consider a particle starting at a distance λ from the origin. Then the $\hat{y}$ direction flux due to particles originating from both sides of disk is:

$$P(\theta, \phi) = 2\int_{-\infty}^{0} (m_i v_z)[N_i v_y f(v_r) dv_r] \tag{2.4}$$

where v_z is velocity in $\hat{z}$ direction, v_r is the velocity in radial direction and $f(v_r)$ is the velocity distribution in radial direction (Maxwellian).

Since the local magnetic field is a random function over space; we need to average out the above flux to get mean stress. We get the hybrid viscosity to be:

$$\eta_{hyb} = -\frac{P}{u'(0)} = \frac{2}{15} m_i N_i \lambda \sqrt{\frac{2kT_i}{\pi m_i}} \tag{2.5}$$

2.2 Two Temperature Accretion Disk Model

We consider a quasi-keplerian, steady state disk. The ions and electrons are assumed to be coupled only by Coulomb collisions. The electrons are at a temperature, T_e and radiate away energy via inverse Compton scattering. The underlying assumption is that inter-species interactions happen at a much lower timescales than intra-species. That is the ions get enough time to come to an equilibrium temperature but do not get sufficient time to equilibrate with electrons before they are swept away into the black hole, i.e.,

$$t_{ei} > t_{accr} > t_{ii} > t_{ee}$$

A model based on the basic structure equations, 1.9-1.13, derived in the previous chapter is discussed in detail in SBK96. They start with a quasi-keplerian disk, with $T_i \gg T_e$. The viscosity parameter α is obtained from the hybrid viscosity found in eq 2.5. They work on the assumption that magnetic coherence length varies in a self-similar manner with local height, H.

$$\boxed{\lambda_{coh} = \xi H} \tag{2.6}$$

where ξ is a free parameter, taken to be a constant for a particular model.
With the above constraints on temperature and making the disk structure equations dimensionless by substituting, $M_8 = \frac{M}{10^8 M_\odot}$,$M_* = \dot{M}/1M_\odot\ yr^{-1}$, and $R_* = R/(GM/c^2)$ we get:

$$T_i = 4.99 \times 10^{10}(0.22 \times \frac{\dot{M}_*}{M_E}) f_2 {\tau_{es}}^{-1} \alpha^{-1} {R_*}^{-3/2} \tag{2.7}$$

$$T_e = 1.40 \times 10^9 y {\tau_{es}}^{-1} (1 + \tau_{es})^{-1} \tag{2.8}$$

$$N_i = 4.70 \times 10^{10}((0.22 \times \frac{\dot{M}_*}{M_E}))^{\frac{1}{2}} \dot{M}_*^{-1} f_1^{1/2} f_2^{-1/2} {\tau_{es}}^{3/2} \alpha^{1/2} {R_*}^{-3/4} \tag{2.9}$$

The viscosity parameter α is defined by shear stress as

$$\alpha_{hyb} = -\eta_{hyb} R \frac{d\Omega_{kep}}{dR} \tag{2.10}$$

With the above parameters, the following equations give a self consistent solution for the model:

$$\alpha_{hyb} = 147.31 \delta^{1/3} f_1^{-1/6} f_2^{2/3} (0.22 \times \frac{\dot{M}_*}{M_E})^{2/3} \tau_{es}^{-1} R_*^{-1} \tag{2.11}$$

$$T_i = 3.38 \times 10^{11} \delta^{-1/3} f_1^{1/6} f_2^{1/3} (0.22 \times \frac{\dot{M}_*}{M_E})^{1/3} R_*^{-1/2} \tag{2.12}$$

$$T_e = \frac{1.40 \times 10^9 y}{\tau_{es}(1+\tau_{es})} \tag{2.13}$$

$$N_i = 5.70 \times 10^{11} \delta^{1/6} f_1^{5/12} f_2^{-1/6} (0.22 \times \frac{\dot{M}_*}{M_E})^{5/6} ((\dot{M})_*)^{-1} \tau_{es} (R_*)^{-5/4} \tag{2.14}$$

$$\frac{H}{R} = 0.175 \delta^{-1/6} f_1^{5/12} f_2^{1/6} (0.22 \times \frac{\dot{M}_*}{M_E})^{1/6} R_*^{1/4} \tag{2.15}$$

where the parameter δ is defined as:

$$\delta = \frac{\lambda}{\lambda_{ii}} = (1 + \frac{\lambda_{ii}}{\xi H}) \tag{2.16}$$

Given accretion rate, ξ parameter, and Compton y-parameter, we can determine δ as:

$$\tau_{es} = 915.508 \xi^{-1} \frac{\delta^{1/3}}{1-\delta} f_1^{1/3} f_2^{2/3} (0.22 \times \frac{\dot{M}_*}{M_E})^{2/3} {R_*}^{-1} \tag{2.17}$$

$$\tau_{es}^{7/3}(1+\tau_{es}) = 57.8819 \delta^{\frac{1}{9}} f_1^{-7/18} f_2^{-1/9} f_3^{2/3} y (0.22 \times \frac{\dot{M}_*}{M_E})^{5/9} {R_*}^{-5/6} \tag{2.18}$$

2.2.1 Ion Inertial length as Magnetic Coherence Length

The treatment of SBK96 assumed the ratio of the magnetic field coherence length to the disk height to be a free parameter, which is not a realistic approximation. In this work, we proposed to use ion inertial length as the magnetic coherence length. Going back to the assumptions, notice that we have a tangled but frozen magnetic in plasma medium, and practically no interaction between ions and electrons. Ion inertial length provides us with the most general length scale to be considered for magnetic coherence length. This prescription for the effective mean free path has been used to compute the operative viscosity in the collisionless solar wind [7], [8].

$$\boxed{\lambda_{coh} = \frac{c}{\omega_p} \sim 2.28 \times 10^7 N_i^{-\frac{1}{2}} \mathrm{cm}} \tag{2.19}$$

With the above prescription, we now have ξ parameter as:

$$\xi = 2.28 \times 10^7 N_i^{-\frac{1}{2}} H^{-1} = \frac{2.28 \times 10^7 \sigma_T N_i^{1/2}}{\tau_{es}} \tag{2.20}$$

That is, a ξ which also depends on local ionic density.

We solve the equations for the above model, with this new parametrization and observe the changes and compare the two models. The new disk parameters are governed by the following equations.

Using above and equation 3.12 with equation 2.17 to substitute ξ give us the following equation:

$$\tau_{es}^{1/2} = 8.651 \times 10^9 \frac{\delta^{1/4}}{1-\delta} f_1^{1/8} f_2 (0.22 \times \frac{\dot{M}_*}{M_E})^{1/4} \dot{M}_*^{1/2} R_*^{-3/8} \tag{2.21}$$

Solving equation 2.17 for δ gives:

$$\delta = (57.8819)^9 \tau_{es}^{21/3} (1+\tau_{es})^9 f_1^{7/2} f_2 f_3^{-6} y^{-1} (0.22 \times \frac{\dot{M}_*}{M_E})^{-5} R_*^{15/2} \tag{2.22}$$

Substituting for δ in the equation 2.21 for τ gives us an implicit equation for τ_{es};
if

$$f(\tau) = 1 - (57.8819)^9 \tau^{21/3} (1+\tau)^9 f_1^{7/2} f_2 f_3^{-6} y^{-1} (0.22 \times \frac{\dot{M}_*}{M_E})^{-5} R_*^{15/2}$$

and

$$g(\tau) = 8.651 \times 10^9 f_1 f_2 f_3^{-3/2} (0.22 \times \frac{\dot{M}_*}{M_E})^{-1/2} \dot{M}_*^{1/8} R_*^{3/2} [\tau^{19/4} (1+\tau)^{9/4}]$$

Then we can get τ_{es} from:

$$\frac{g(\tau_{es})}{f(\tau_{es})} = 1 \tag{2.23}$$

and subsequently we can solve equations 2.11-2.15 for δ, α, ionic density and other such parameters.

2.3 Results and inferences

We have solved the model for a black hole of mass, 10^8 $M_\odot$ and Compton parameter, $y = 1$. The legends on each graph are the accretion rates as a ratio to Eddington rate, $(\frac{\dot{M}_*}{M_8})$.

The following figures give an idea of how various parameters vary as a function or radius of accretion disk.

Following important conclusions can be drawn from the results:

- The parameter α which is usually expected to be in the range of 10^{-4} - 1 comes out to be too small to have any significant effect on the disk structure.
- In the Model discussed in SBK-96, ξ as an external parameter is taken to be around $\sim 10^{-1}$ for a realistic disk model while solving for ξ self-consistently from this model gives it to be very insignificant, which is a big red flag.

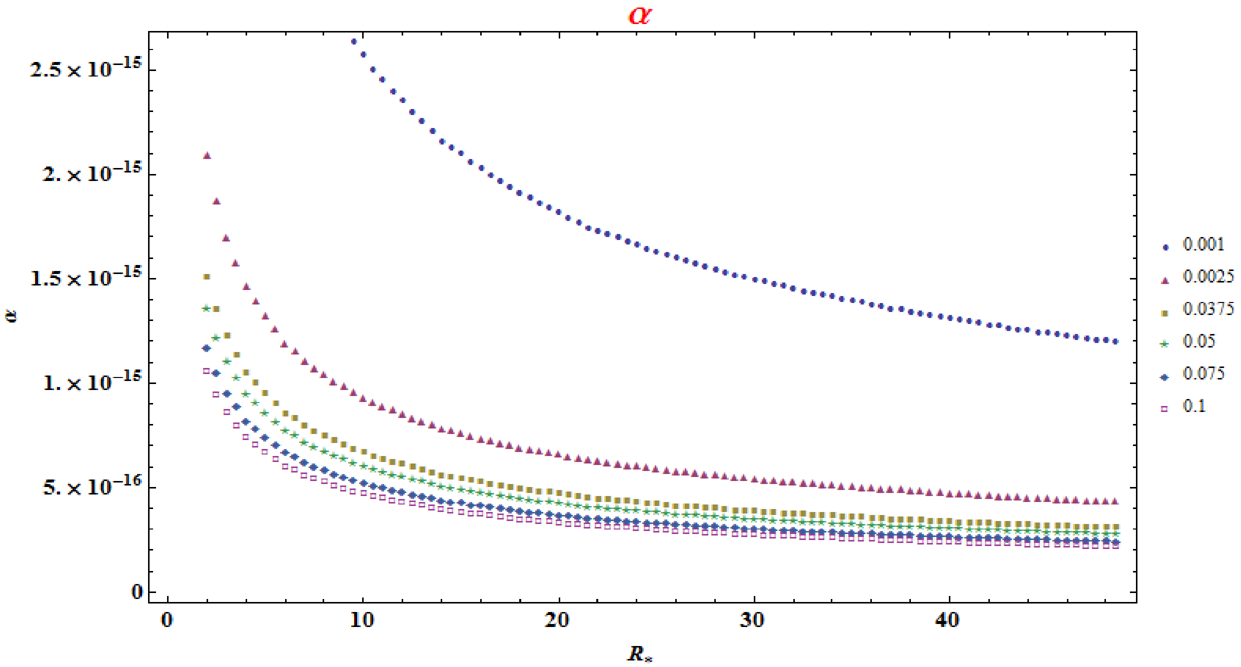

Figure 2.1: α for different accretion rates

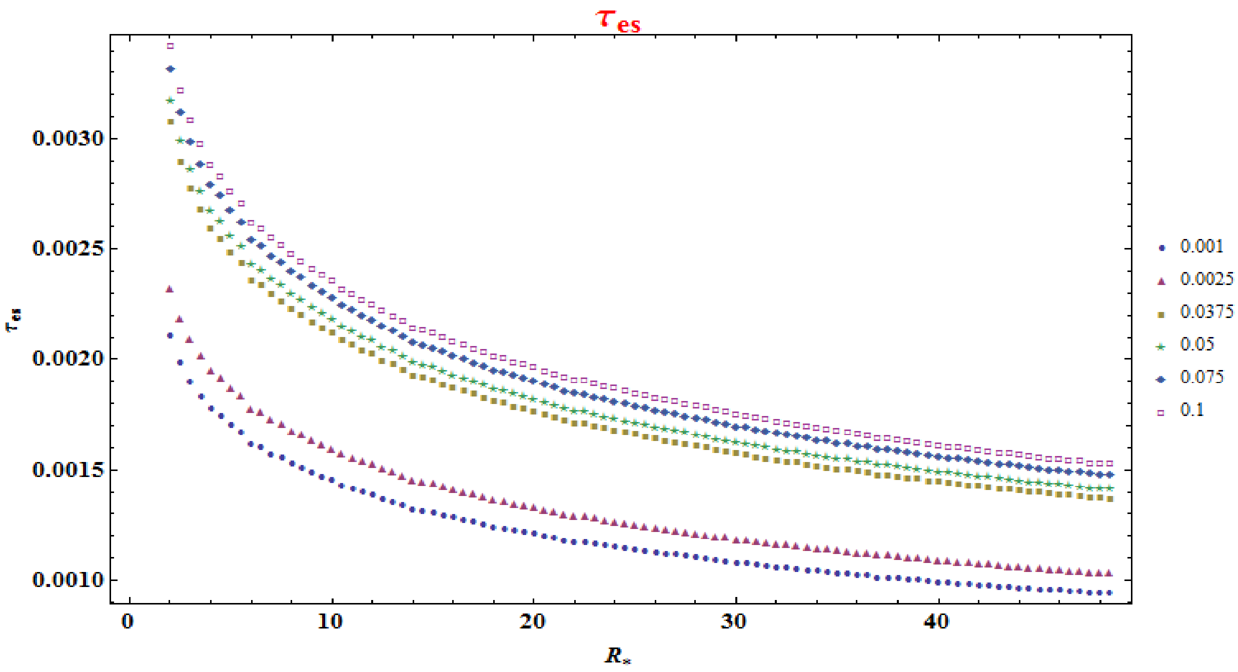

Figure 2.2: τ_{es} for different accretion rates

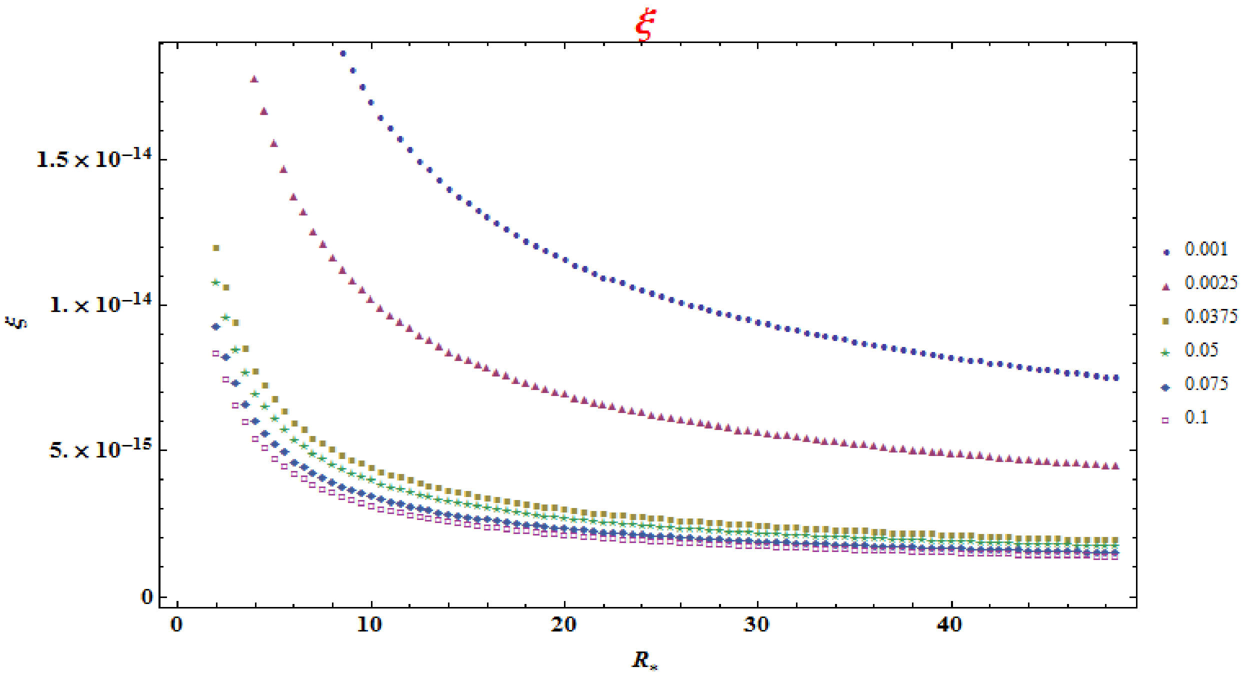

Figure 2.3: ξ for different accretion rates

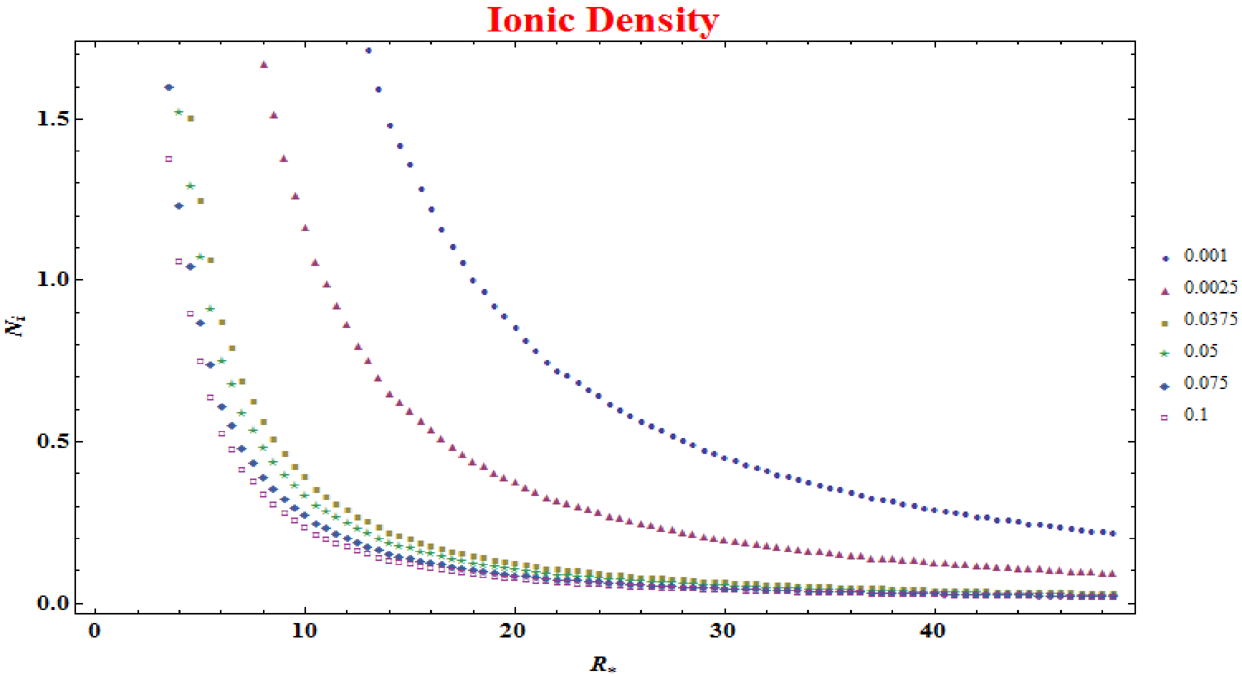

Figure 2.4: N_i for different accretion rates

Chapter 3

VISCOSITY DUE TO DIFFUSION OF CHARGED PARTICLES THROUGH MAGNETIC FIELDS

We see that the model we study in the previous chapter doesn't give a realistic picture of an accretion disk. Recent studies have shown that a large-scale toroidal field is expected in the disk along with the random turbulent magnetic components, or 'kinks'. The earlier picture does not take into account the possibility of any such field. We are also not limited to a fixed length scale fluctuations as opposed to ξ , giving the freedom to take into account all magnetic irregularities below the maximum possible length, L_{max}. With these considerations in mind, we look at other sources to direct us towards a more comprehensive picture.
Transport of ions across turbulent magnetic fields has been studied extensively by people in the context of cosmic rays. We follow one such recent work by Candia and Roulet, 2004 [9]. We will look at the kind of viscosity which arises out of ions diffusing across turbulent magnetic fields. Candia and Roulet perform Monte-Carlo simulations to get diffusion coefficients in of such ions in the presence of a tangled magnetic fields and various levels of turbulence.

3.1 Transport coefficients

Consider a particle moving in a large-scale uniform regular magnetic field, B_o. It follows a helical path with Larmor radius:

$$r_L = \frac{pc}{ZeB_o} \tag{3.1}$$

Now assume a random magnetic field, B_r, with the maximum scale of turbulence as L_{max}. So the net magnetic field is taken of the form,

$$B_R = B_o\hat{z} + B_r(r)$$

The particles will scatter off these 'kinks' without changing their velocities (only direction). In general the diffusion tensor is written as:

$$D_{ij} = (D_{\parallel} - D_{\perp})b_i b_j + D_{\perp}\delta_{ij} + D_A \epsilon_{ijk} b_k \tag{3.2}$$

here, $\vec{b} = \vec{B_o}/B_0$ is a unit vector in the direction of large-scale magnetic field. A large sample of configuration on random magnetic field is generated and then the trajectory of the particle following net field is followed. This is averaged over a large number of different field configurations and in different directions to provide a diffusion constant.
The different levels of turbulence are defined by $\sigma^2 \equiv \frac{<B_r^2>}{B_o^2}$. For details refer Candia and Roulet, 2004 [9].

3.2 Hybrid Viscosity

Most simulations of the magnetorotational instability (MRI) in accretion disks reveal a large-scale toroidal magnetic field embedded in the disk, together with turbulent irregularities. In our case, we are looking at momentum transport in the radial direction; i.e., across the large-scale toroidal field in the presence of turbulent magnetic field fluctuations. Motion of particles in perpendicular direction to the large-scale magnetic field is what makes momentum flux flow across the disk. So we use the perpendicular component of diffusion constant, $D_{\perp}$ to characterize the mean free path of ions. This was initially suggested by Subramanian, Becker, Kafatos 2005 [10].

We directly borrow the analytical fit given by Candia and Roulet, for $D_\perp$.

$$D_\perp = v_{rms} L_{max} D_c \tag{3.3}$$

Here,

$$D_c = N_\perp (\sigma^2)^{a_\perp} \rho \frac{N_\parallel}{\sigma^2} ((\frac{\rho}{\rho_\parallel})^{2(1-\gamma)} + (\frac{\rho}{\rho_\parallel})^2)^{1/2} \tag{3.4}$$

where σ^2, as defined, gives the level of turbulence in magnetic field, ρ denotes rigidity, and other factors are determined by the type of turbulence used in the simulation. v_{rms} is the velocity of thermalized protons. L_{max}, or the Larmor radius is taken to be radius, R of the disk.

In it's most general form, coefficient of dynamic viscosity can be defined as, $\eta = Nm\lambda$ ($gcm^{-1}s^{-1}$). Nm is the mass density of the particles in question and λ is the mean free path.

On the other hand, diffusion constant, D, is defined as $D = v\lambda$ (cm^2s^{-1}). Combining these we get:

$$\eta = NmD$$

Or in case of hot protons, dynamic viscosity arising out of radial transport perpendicular to magnetic field:

$$\eta_{hyb} = N_i m_p D_\perp \tag{3.5}$$

Substituting for $D_\perp$ and m_p and using equation of state, (equation 1.6) we get:

$$\boxed{\eta_{hyb} = 2.511 \tau_{es} v_{rms} D_c \times \frac{R}{H}} \tag{3.6}$$

Using this new definition of coefficient of viscosity, we would like to see how it affects the same two-temperature disk model we discussed earlier with the previous η_{hyb}.

3.3 Two-Temperature Accretion Disk Model

To get the disk structure equations, we solve for α_{hyb}, using equation 2.10, with η_{hyb} as in the previous section.

$$\alpha_{hyb} P = -\eta_{hyb} R \frac{d\Omega_{kep}}{dR} \tag{3.7}$$

Using $\Omega_{kep} = \sqrt{\frac{GM}{R^3}}$ and equation 1.6 for pressure, P we get: (After substituting to make it dimensionless)

$$\alpha_{hyb} = 1.4161 f_2^{-1} \tau_{es}\, D_c^2\, (0.22 \times \frac{\dot{M}_*}{M_E})^{-1} M_8^{-2} R_*^{1/2} \tag{3.8}$$

We can solve for other disk parameters like temperature, ion density, etc. using the following:

$$\tau_{es} = 7.85 \times 10^{-4}\, f_1^{-1/5} f_2^{2/5} f_3^{2/5}\, y^{3/5}\, R_*^{-1/5}\, D_c^{2/5} M_8^{-2/5} \tag{3.9}$$

$$T_i = 4.99 \times 10^{10} (0.22 \times \frac{\dot{M}_*}{M_E}) f_2 {\tau_{es}}^{-1} \alpha^{-1} {R_*}^{-3/2} \tag{3.10}$$

$$T_e = 1.40 \times 10^9 y {\tau_{es}}^{-1} (1 + \tau_{es})^{-1} \tag{3.11}$$

$$N_i = 4.70 \times 10^{10} (0.22 \times \frac{\dot{M}_*}{M_E})^{\frac{-1}{2}} M_8^{-1} f_1^{1/2} f_2^{-1/2} {\tau_{es}}^{3/2} \alpha^{1/2} {R_*}^{-3/4} \tag{3.12}$$

$$\frac{H}{R} = 0.1014\, \tau_{es}\, (R_*\, N_i\, M_8)^{-1} \tag{3.13}$$

Notice that we have the optical depth, τ_{es}, and hence ionic density, N_i and H/R independent of accretion rate. We have an almost self consistent disk model with only external parameters being, turbulence level σ^2, ρ and accretion rate, $(0.22 \times \frac{\dot{M}_*}{M_E})$. Rigidity, ρ is defined as the ratio between Larmor radius and the maximum scale length $\rho = \frac{r_L}{L_{max}}$. L_{max} could be taken as either be H or R (minimum of both).

σ^2 is varied from 0.01 to 1 which covers low to high levels of turbulence. Similarly, ρ is also varied from 0.01 to 1 and the optimum value is taken. Here 'optimum' value is mostly defined by realistic ion temperature. Higher temperature correlates with lower values of σ^2 and ρ.

3.4 Results

We solved the above equations for Kraichnan and Kolmogorov processes with the parameters given below:

Spectrum	γ	$N_{\parallel}$	$\rho_{\parallel}$	$N_{\perp}$	$a_{\perp}$
Kraichnan	$^3/_2$	2.0	0.22	0.019	1.37
Kolmogorov	$^5/_3$	1.7	0.20	0.025	1.36

The Ionic temperature keeps on increasing with accretion rate. We notice that for accretion rates $(0.22 \times \frac{\dot{M}_*}{M_E}) > 0.001$*, the temperature goes above* 10^{13} *K at which ions cannot be in a thermal equilibrium, so we take it as an upper limit for our model, that is we take this prescription to be valid only for underfed accretion disks. (Fig. 3.1)*

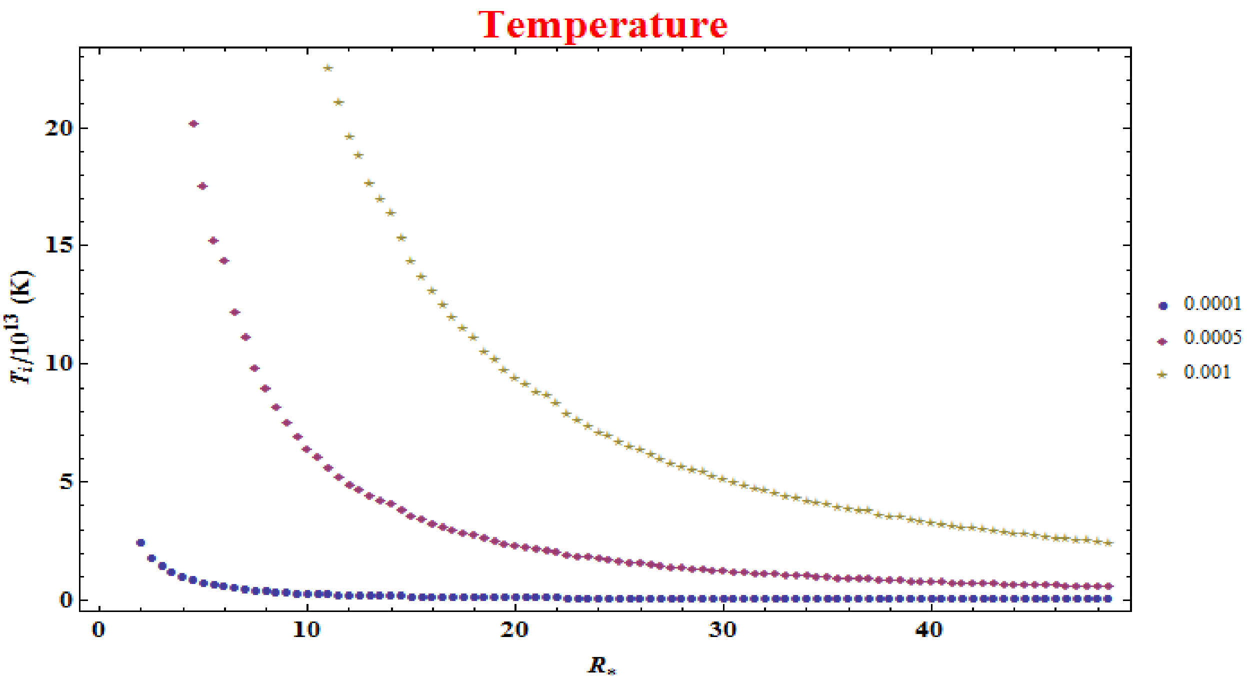

Figure 3.1: T_i for Kolmogorov process for accretion rates of 0.0001, 0.0005, and 0.001.

There are following important observations about the disk from the numerical analysis:

- We have optical depth, $\tau_{es} \sim 10^{-4}$ independent of the accretion rate, hence remains constant, albeit optically thin. Fig 3.3
- The ion temperature is high. It increases with increasing the accretion rate giving an upper cut off for accretion rate. Fig 3.4
- As we can see, H/R value is of the order $\sim 10^5$, that is the disk is not a thin disk, rather it's puffed up. It also clears up that turbulent magnetic length scale, L_{max} should be

taken as R, not H. This is also independent of accretion rate, which is interesting. Fig 3.5

- We can see from the figures 3.6, 3.7, 3.8, 3.9, that the Kraichnan parameters result in rather unrealistic disk structure. The temperature it leads to completely unreasonable. In the following discussions we will only consider the Kolmogorov spectrum.

Following figures give some disk structure parameters for Kolmogorov and Kraichnan turbulence for accretion rates, 0.0001, 0.0005 and 0.001, keeping below our upper cut-off, for a black hole of mass $10^8 M_\odot$.

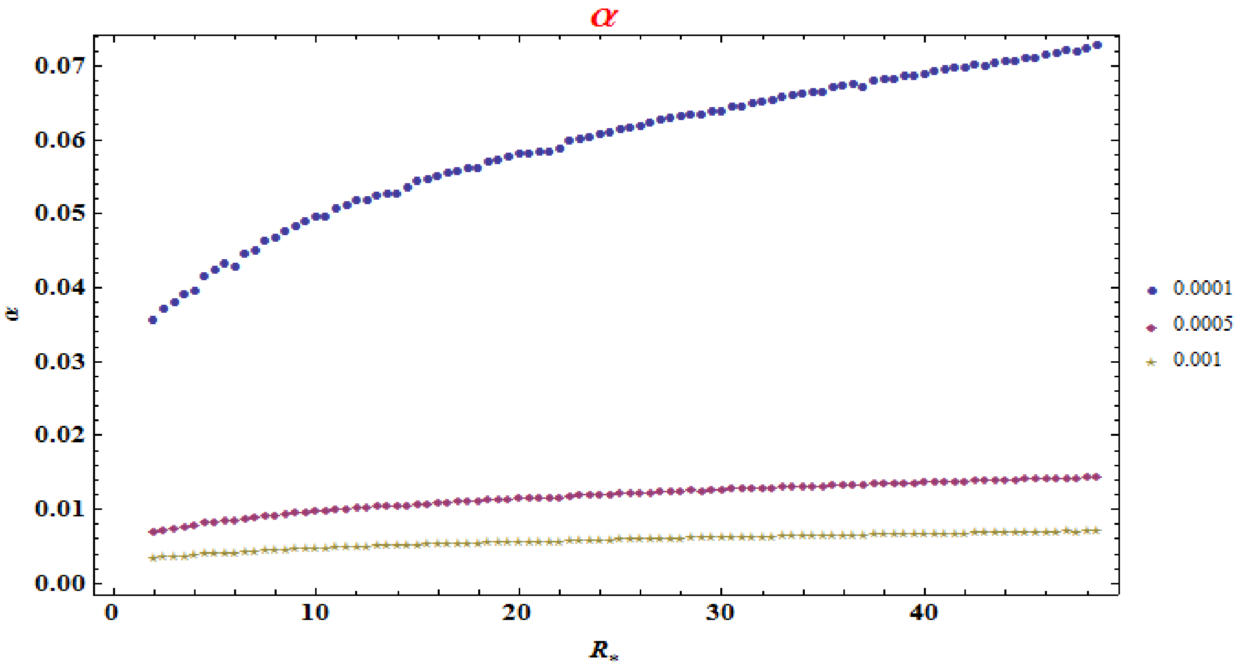

Figure 3.2: α for Kolmogorov process for the given accretion rates of 0.0001, 0.0005, and 0.001.

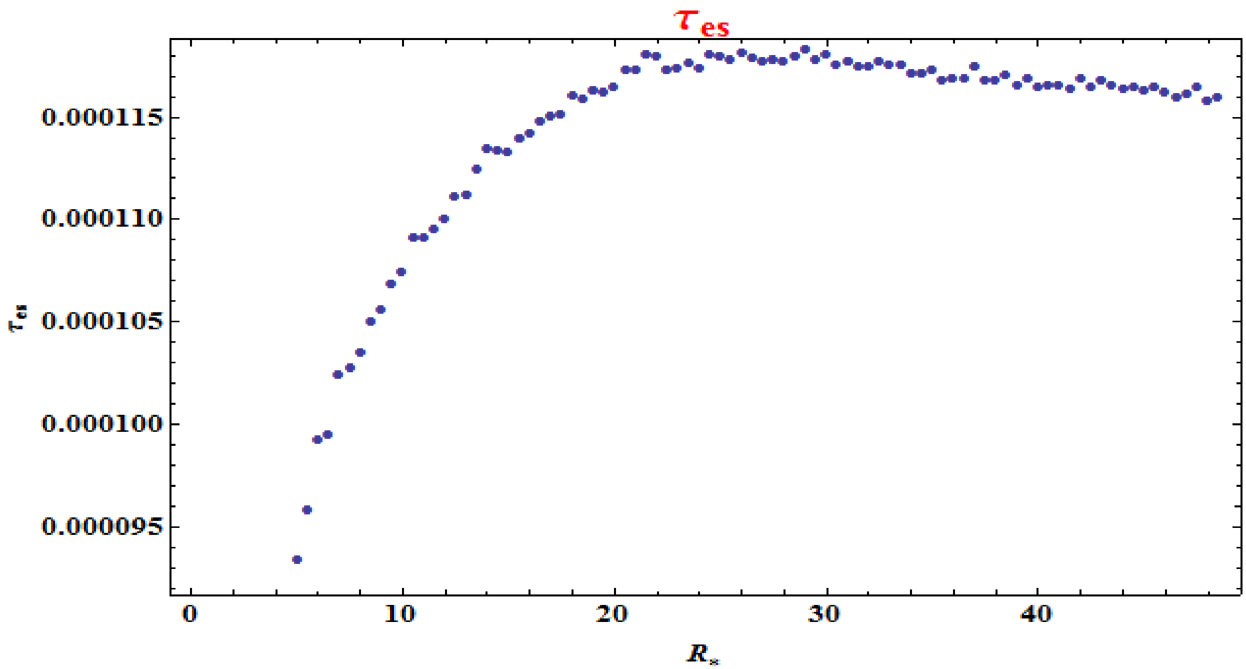

Figure 3.3: τ_{es} for Kolmogorov spectrum (Independent of accretion rate).

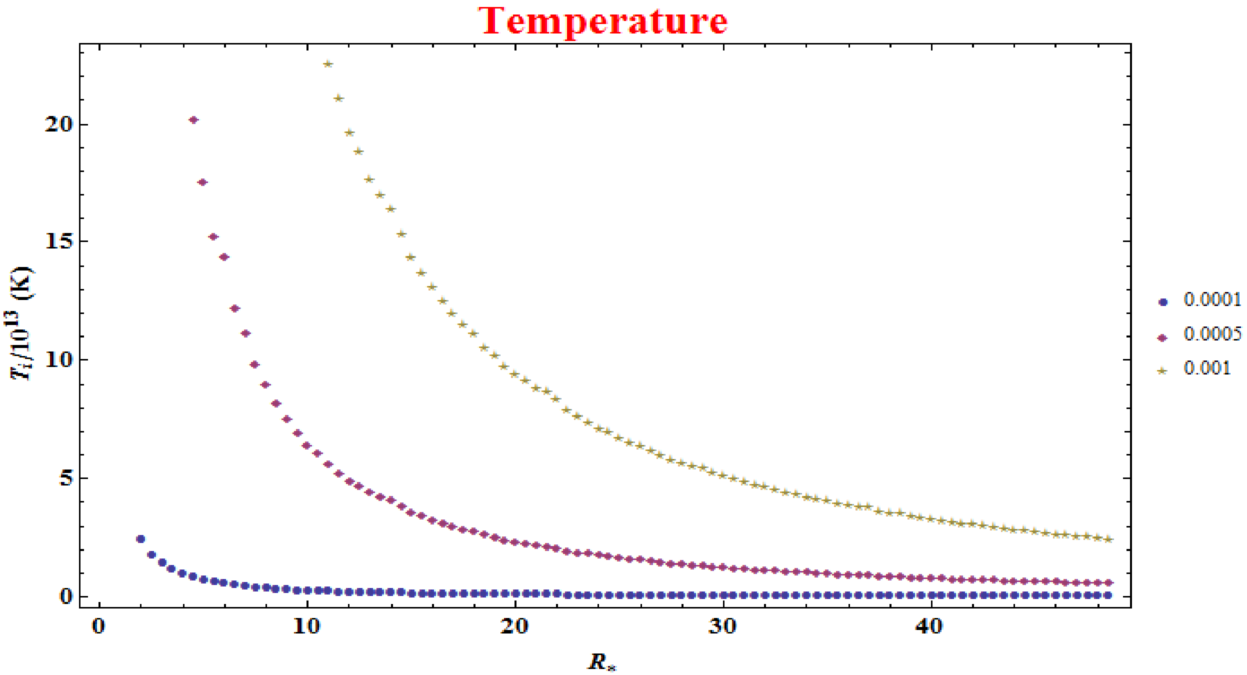

Figure 3.4: Kolmogorov Spectrum: Temperature/10^{13} for different accretion rates

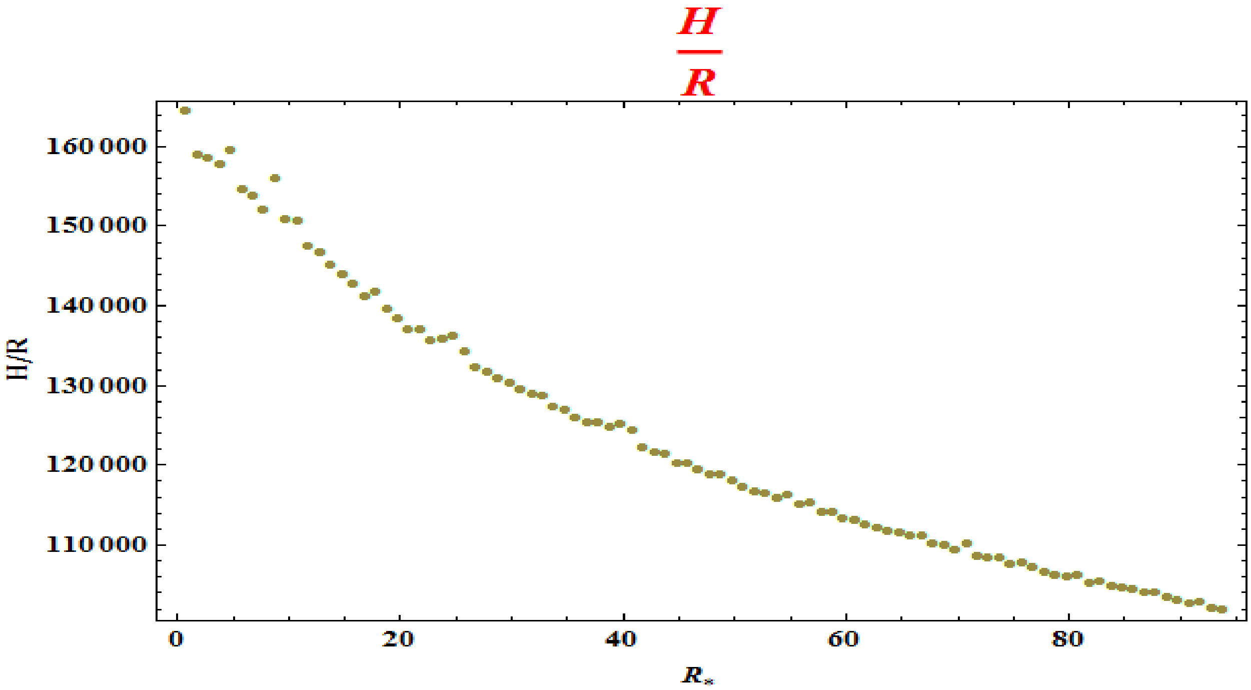

Figure 3.5: Kolmogorov Spectrum: $\frac{H}{R}$ (Independent of accretion rate)

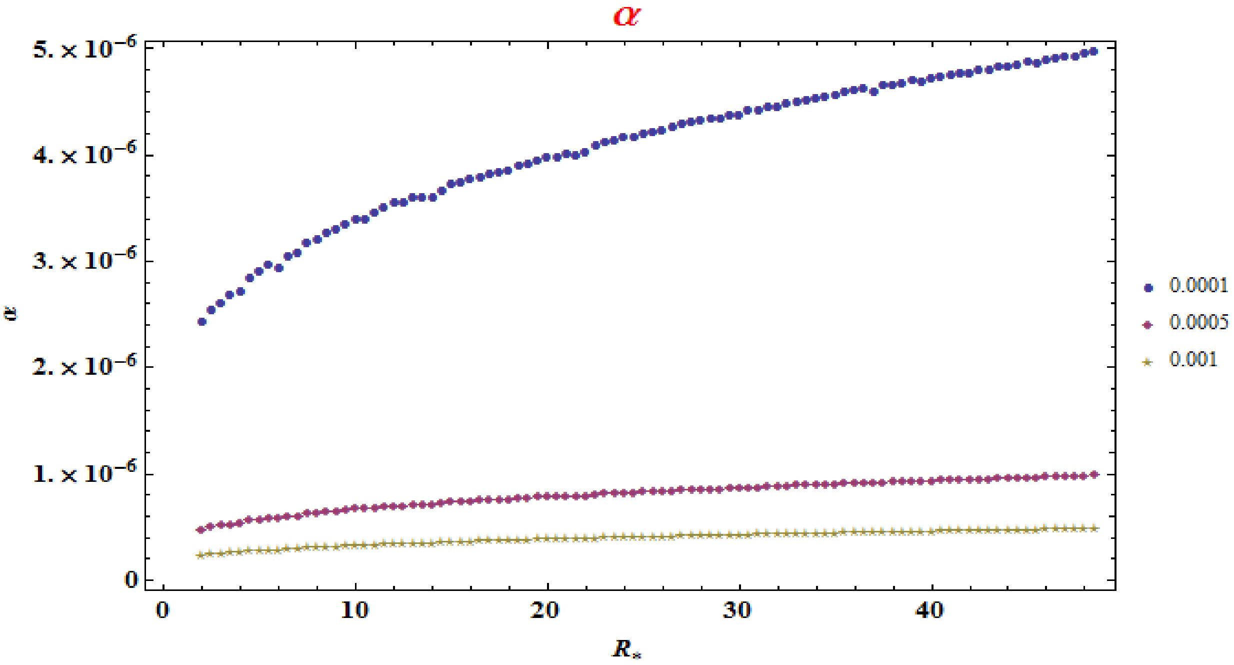

Figure 3.6: Kraichnan Spectrum: α for different accretion rates

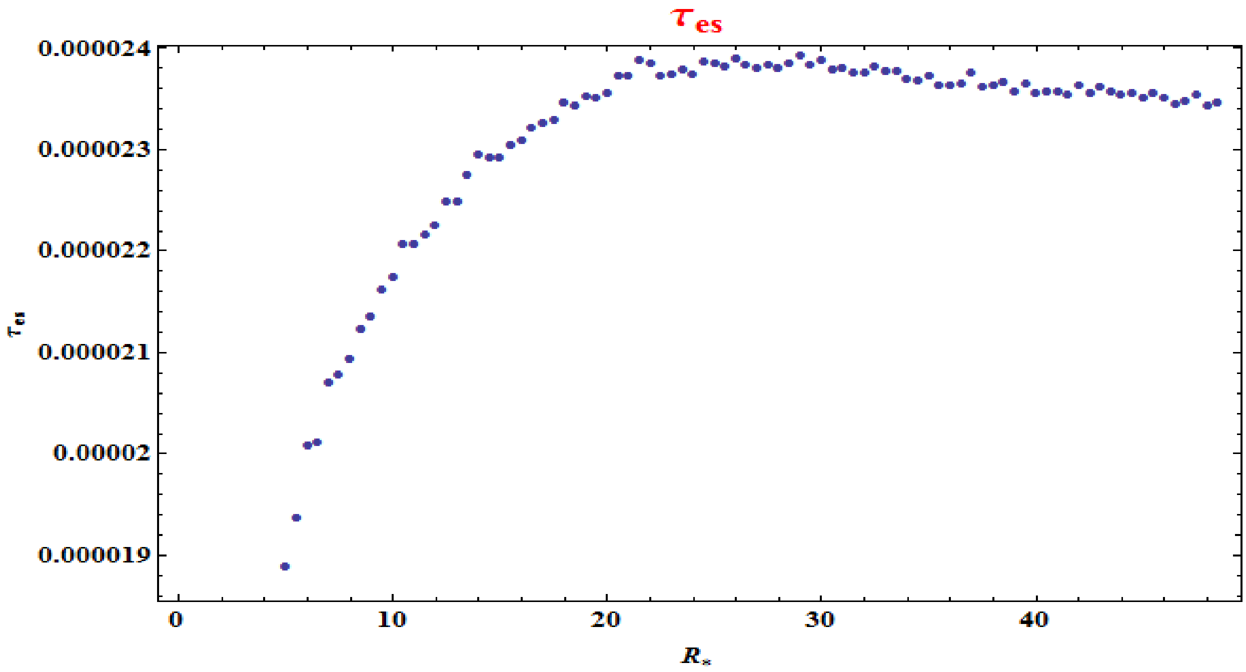

Figure 3.7: τ_{es} for Kraichnan spectrum (Independent of accretion rate).

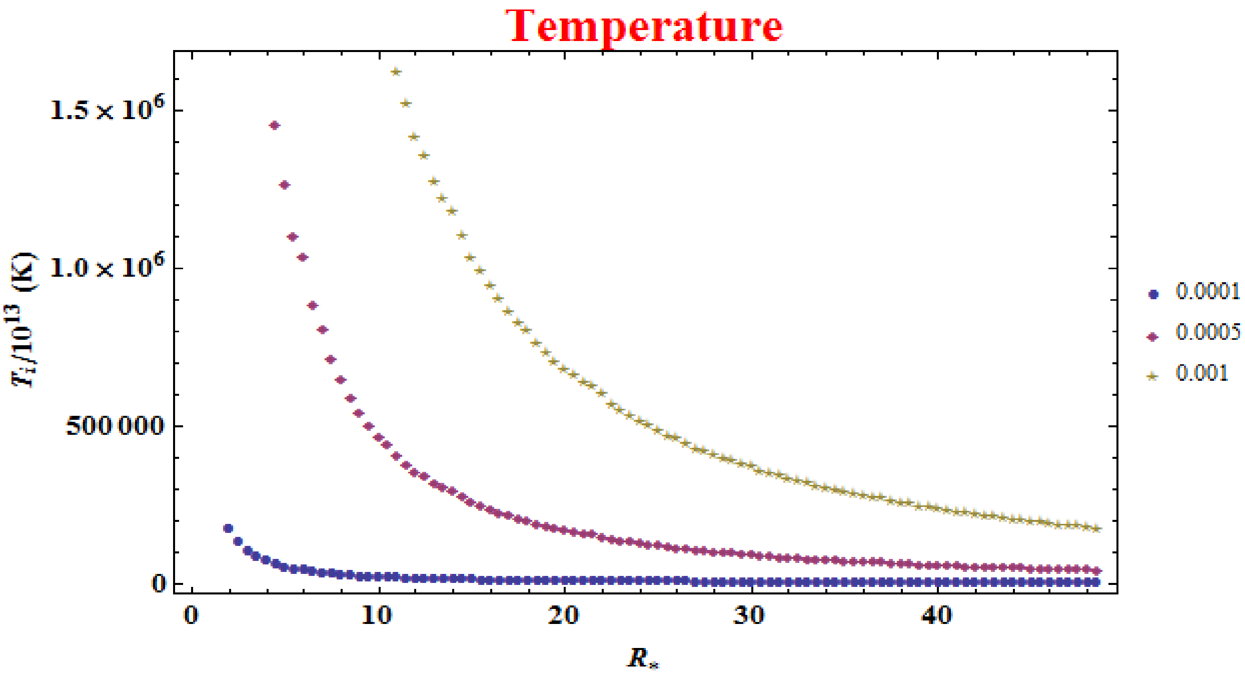

Figure 3.8: Kraichnan Spectrum: Temperature/10^{13} for different accretion rates

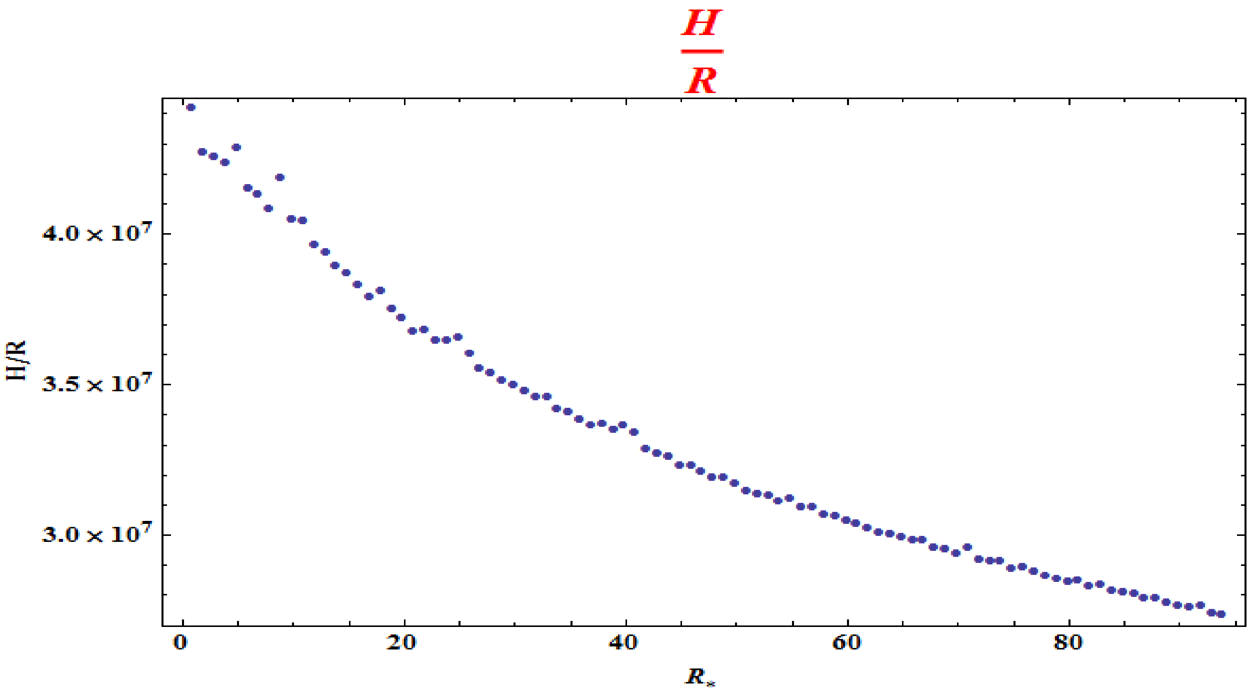

Figure 3.9: Kraichnan Spectrum: $\dfrac{H}{R}$ (Independent of accretion rate).

Chapter 4

Instability of Disk and Viscous timescales

Accretion process has long been connected with phenomena like jet ejections, X-ray variations, etc. Disk instabilities, if any, can be used to explain some of these observed variations. With this motivation, we would like to test the accretion disk model discussed in the previous chapter for stability. There has been a lot of significant work done in discussing an accretion disk's stability, notably by Shakura and Sunyaev, 1976 [11], Piran, 1978 [12]. We follow the general prescription given by Piran to check the stability.

4.1 Disk Instability

The most important factors in deciding if a disk is stable or not are it's dissipation and cooling rate, which are defined by the viscosity and cooling mechanism in play. The stability condition is given as: [12]

$$\left.\frac{d\,ln\,Q^{+}}{d\,ln\,H}\right|_{U} < \left.\frac{d\,ln\,Q^{-}}{d\,ln\,H}\right|_{U} \tag{4.1}$$

where Q^{+}, Q^{-} are the dissipation rate and cooling rate respectively and U($= N_i m_p H$) is the surface density of ions.

To generalize the derivation, the dynamic viscosity, (ν) and cooling rates are described phenomenologically in terms of their logarithmic derivatives with respect to H and U:

$$\nu = \frac{\alpha}{9}\frac{\omega}{{U_o}^n {H_o}^{m-2}} H^m U^n \tag{4.2}$$

and

$$Q^- = \delta \frac{\omega^3}{{U_o}^{l-1} {H_o}^{k-2}} H^k U^l \tag{4.3}$$

where U_o and H_o are steady state values of H and U, and α and δ are dimensionless parameters. k,l,m,n are defined as [12]:

$$k \equiv \left.\frac{d\,ln\,Q^-}{d\,ln\,H}\right|_U; \quad l \equiv \left.\frac{d\,ln\,Q^-}{d\,ln\,U}\right|_H; \quad m \equiv \left.\frac{d\,ln\,\nu}{d\,ln\,H}\right|_U; \quad n \equiv \left.\frac{d\,ln\,\nu}{d\,ln\,U}\right|_H \tag{4.4}$$

To study the temporal behaviour of the disk, we look the energy balance equation and the mass transfer equation:

$$\frac{\partial}{\partial t}E = \frac{P}{\rho^2}\frac{d\rho}{dt} + \frac{Q^+}{U} - \frac{Q^-}{U} \tag{4.5}$$

and

$$\frac{\partial}{\partial t}U = -\frac{1}{R}\frac{\partial}{\partial R}(UV_r R) = \frac{6}{R}\frac{\partial}{\partial R}\frac{1}{\omega R}\frac{\partial}{\partial R}(\nu \omega U R^2) \tag{4.6}$$

We introduce axially symmetric perturbations of the wavelength, Λ. Assuming solutions for U and H as $U = U_o(1+u)$ and $H = H_o(1+h)$, where u and h are small, linearize equation 4.5 and 4.6. In order to look for growing perturbations, we find the dispersion relation with an exponential time dependence. [For details, see Piran [12]]. The solutions of the dispersion relation are:

$$\begin{aligned} \Omega_{\pm} = \frac{3\alpha\omega}{2A}&[[-[2B(\frac{H_o}{3\Lambda})^2 - (1+2\beta_o)(m-k)] \\ &\pm ([2B(\frac{H_o}{3\Lambda})^2 - (1+3\beta_o)(m-k)]^2 + 8A(1+3\beta_o)[ml-(n+1)k](\frac{H_o}{3\Lambda})^2)^{1/2}]] \end{aligned} \tag{4.7}$$

For the perturbations to grow and make the disk unstable, the Re(Ω) should be positive. The stability depends on the signs of the terms in the equation. The necessary conditions for stability comes out to be:

$$m < k \tag{4.8}$$

$$ml < (n+1)k \tag{4.9}$$

In long wavelength limit, with condition 4.8 satisfied, Ω_+ corresponds to the Lightman-Eardley mode and Ω_- to the thermal mode, and vice-versa for $m > k$. When $m > k$, the disk becomes very hot and thermally unstable. Condition 4.9 determines the stability of Lightman-Eardley mode. For detailed analysis, refer Piran, 1978 [12].

4.1.1 Stability of Diffusion based model

To check the stability of our model; we need to calculate m, n, k and l parameters. From equation 3.6, we have

$$\eta_{hyb} = 2.511\tau_{es}v_{rms}D_c$$

so dynamic viscosity (ν) will be:

$$\nu = \eta_{hyb}/\text{mass density} = \eta_{hyb}/N_i m_p = \eta_{hyb}H/U \tag{4.10}$$

v_{rms} is given by $\sqrt{\frac{3k_BT_i}{m_p}}$, and we use equation 1.10 $\tau_{es} = N_i\sigma_T H = \frac{U\sigma_T}{m_p}$. So we get,

$$\nu = 2.511\frac{H}{U}\frac{U\sigma_T}{m_p}H\sqrt{\frac{3k_BT_i}{m_p}} \tag{4.11}$$

From equation 2.7, we know that $T_i \propto \tau_{es}^{-1}$, we finally get:

$$\nu \propto H^2U^{-1/2}$$

Giving us $m = 2$ and $n = -1/2$. For a two temperature disk, main process by which it loses energy is Comptonization, which gives $k = 1$ and $l = 7/2$. Comparing with the stability criterion, we have:

$$m > k$$

and

$$ml > (n+1)k$$

That is the disk in not stable in thermal mode but is stable in Lightman-Eardley mode [13], (viscous perturbations). This signifies that the cooling process is not able to keep up with heat dissipation and the disk temperature increases fast, or the disk is hot, which we have already seen from the temperature profile. In the Lightman-Eardley mode, the disk oscillates with $Q^+ = Q^-$.

4.2 Viscous Timescales and Comparison with Observations

A lot of transient phenomena in astrophysics are thought to take place in viscous timescales, that is timescales at which matter is supposed to move through the disc under the effect of viscous torques. Accretion process powers the black holes, and active galactic nuclei (AGNs) and many of these systems emit radiations and have relativistic jets. We try to compare the timescales at which these happen to the viscous timescale obtained with our model to see if it can hint towards possible disk-jet connections.

4.2.1 Viscous Timescale

The viscous timescale or the time which a small disk annulus takes to reach radius R is given by [14]:

$$t_{visc} \sim \frac{R^2}{\nu} \tag{4.12}$$

We had the dynamic viscosity as:

$$\nu = \frac{\eta_{hyb}}{N_i m_p} = D_\perp = v_{rms} H D_c \tag{4.13}$$

$$\Rightarrow \nu = 0.2367 \times 10^{29} \, T_i^{1/2} \tau_{es} \, N_i^{-1} D_c \tag{4.14}$$

Substituting $R_* = R(GM/c^2)$ in equation 4.12:

$$\boxed{t_{visc} = 0.928 \times 10^{-2} \, R_*^2 \, M_8^2 \, T_i^{-1/2} (\tau_{es} D_c)^{-1} N_i} \tag{4.15}$$

We will use the above expression from here on to calculate viscous time while comparing with observations. Following graph give viscous timescales (in seconds) for Kolmogorov process (Fig 4.1).

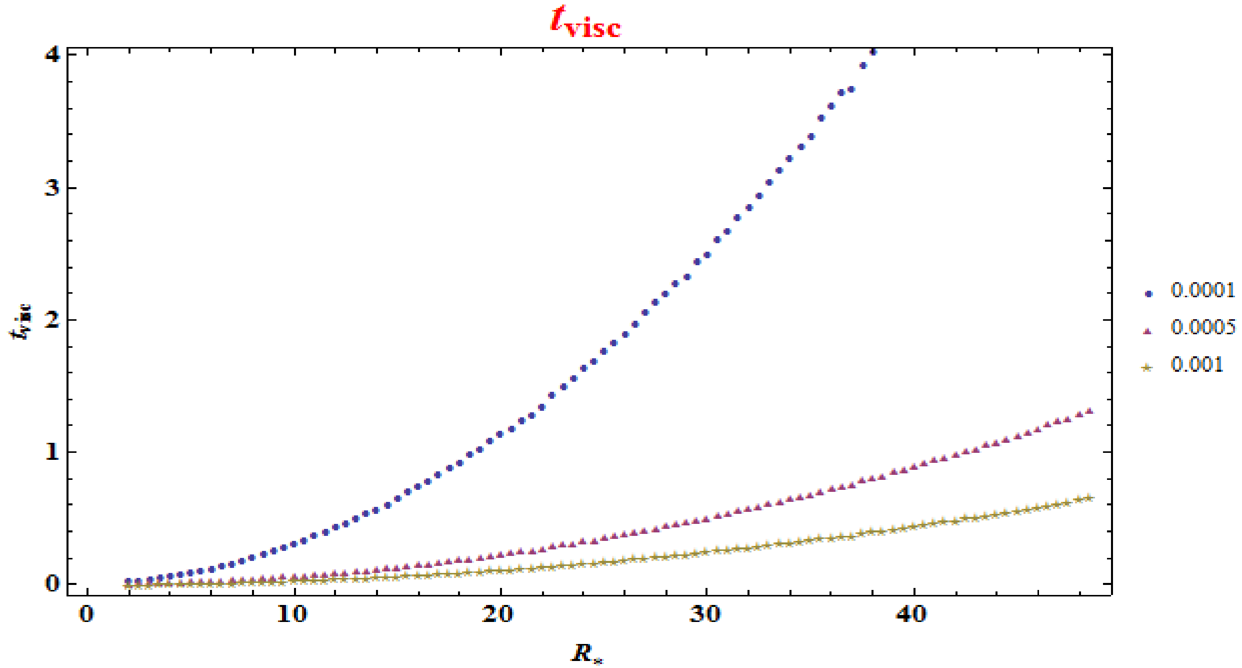

Figure 4.1: t_{visc} for Kolmogorov process for different accretion rates

4.2.2 Observations

Active Galactic Nuclei (AGNs) and Black hole X-ray binaries (BHXRBs) are powered by accretion onto black hole and emit radiation and relativistic jets. We follow the work done by Chatterjee, et al. [2], where they have presented the results of monitoring of active radio galaxy 3C 120 between 2002 and 2007 in X-ray, optical and radio wave bands. The system exhibits an interesting correlation and anti-correlation between X-ray dips and optical and X-rays and radio emissions respectively. Most of the X-rays are produced in the immediate vicinity of the accretion disk, in corona, via hot wind or at the base of the jet, and the correlations between radio emissions, jets might suggest related origins for radio jets. Following are the significant results from the observations [2]:

- X-rays lead the radio variation by 120 ± 30 days. X-ray dips are followed by the appearance of superluminal knot and hence enhancement in 37 GHz flux.

- We can say the decrease in X-ray production is linked with an increase in speed in jet flow, causing a shock front to move downstream.
- X-ray variations lead optical by 0.5 ± 4 days.
- X-rays are produced close to the center of the disk by viscous heating, along with UV, which is then Compton scattered by disk phtons that reach corona to form hard X-ray spectrum in AGN. Part of these X-rays reheats the disk to produce more thermal photons.

We take the time of X-ray dips and compare it to our viscous timescale. The mass of galaxy is taken to be $10^7\ M_{\odot}$. Fig. 4.2 gives the observed data for X-rays dips from 3C 120. The time period of X-ray dips varies greatly with maximum period of $t_{max} = 120$ days to minimum of just $t_{min} = 5$ days with an average of $t_{avg} = 45.3$ days.
The accretion rate in this AGN is supposed to be near Eddington, i.e, $\frac{\dot{M}}{M_E} \sim 1$, but since we are restricted a maximum accretion rate of $\frac{\dot{M}}{M_E} \sim 0.001$, we optimize other parameters, σ^2 and ρ to get near observed timescale. The viscous time is though not very sensitive to either σ^2 or ρ. It increases slightly with increase in these parameters, so we take the maximum allowed values when comparing with observed time.
The figures, 4.3, 4.4, 4.5 give the expected value vs observed time to compare.

4.2.3 $\mathcal{M}_\phi$ Mach number

We also calculate azimuthal Mach number which the medium is likely to have with the above parameters. Azimuthal mach number is defined as[14]:

$$\mathcal{M}_\phi = \frac{v_\phi}{c_s} \tag{4.16}$$

Where $v_{phi} = \sqrt{\frac{GM}{R}}$ is keplerian angular velocity and $c_s = \sqrt{\frac{P}{\rho}}$ is the speed of sound in the medium. We get mach number, $\mathcal{M}_\phi$ to be:

$$\mathcal{M}_\phi = 3.300 \times 10^6 \, (T_i \, R_*)^{-1/2} \tag{4.17}$$

Fig. 4.6 give mach number for Kolmogorov process.
The flow is mostly subsonic and seems to reach supersonic only for very low accretion rates.

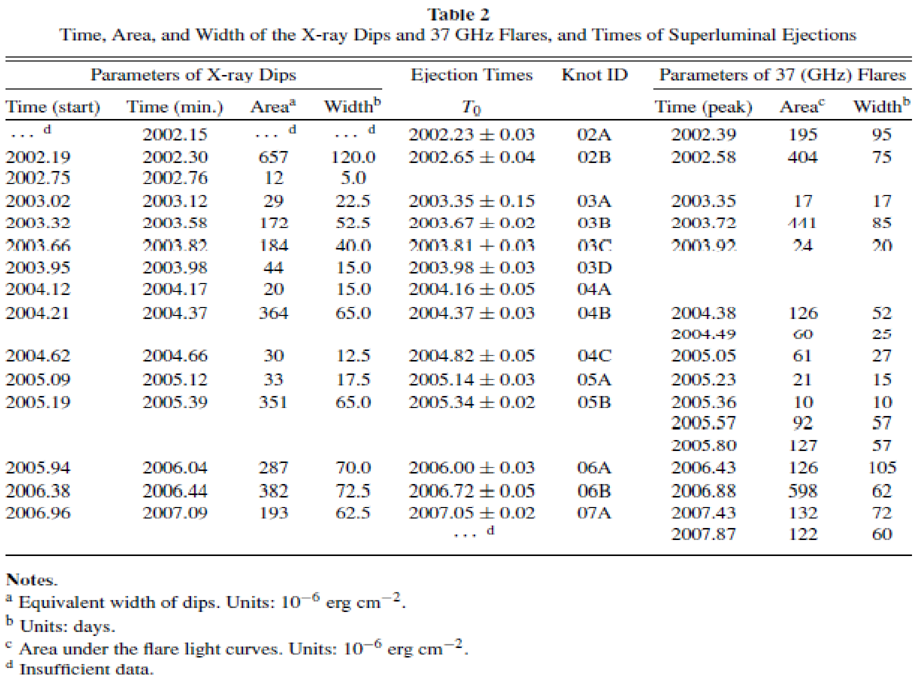

Table 2

Time, Area, and Width of the X-ray Dips and 37 GHz Flares, and Times of Superluminal Ejections

Parameters of X-ray Dips				Ejection Times	Knot ID	Parameters of 37 (GHz) Flares		
Time (start)	Time (min.)	Area^a	Width^b	T_0		Time (peak)	Area^c	Width^b
…^{d}	2002.15	…^{d}	…^{d}	2002.23 ± 0.03	02A	2002.39	195	95
2002.19	2002.30	657	120.0	2002.65 ± 0.04	02B	2002.58	404	75
2002.75	2002.76	12	5.0					
2003.02	2003.12	29	22.5	2003.35 ± 0.15	03A	2003.35	17	17
2003.32	2003.58	172	52.5	2003.67 ± 0.02	03B	2003.72	441	85
2003.66	2003.82	184	40.0	2003.81 ± 0.03	03C	2003.92	24	20
2003.95	2003.98	44	15.0	2003.98 ± 0.03	03D			
2004.12	2004.17	20	15.0	2004.16 ± 0.05	04A			
2004.21	2004.37	364	65.0	2004.37 ± 0.03	04B	2004.38	126	52
						2004.49	60	25
2004.62	2004.66	30	12.5	2004.82 ± 0.05	04C	2005.05	61	27
2005.09	2005.12	33	17.5	2005.14 ± 0.03	05A	2005.23	21	15
2005.19	2005.39	351	65.0	2005.34 ± 0.02	05B	2005.36	10	10
						2005.57	92	57
						2005.80	127	57
2005.94	2006.04	287	70.0	2006.00 ± 0.03	06A	2006.43	126	105
2006.38	2006.44	382	72.5	2006.72 ± 0.05	06B	2006.88	598	62
2006.96	2007.09	193	62.5	2007.05 ± 0.02	07A	2007.43	132	72
				…^{d}		2007.87	122	60

Notes.

[a] Equivalent width of dips. Units: 10^{-6} erg cm^{-2}.

[b] Units: days.

[c] Area under the flare light curves. Units: 10^{-6} erg cm^{-2}.

[d] Insufficient data.

[2]

Figure 4.2: X-ray dip observations for 3C 120

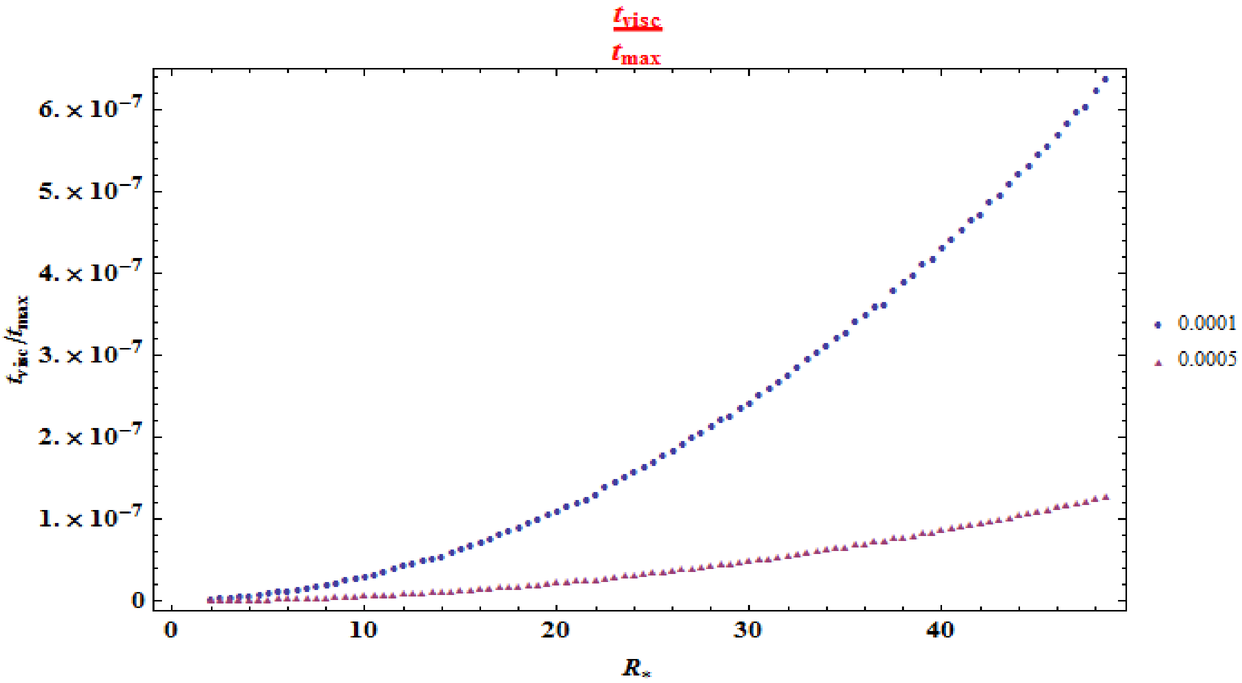

Figure 4.3: $\frac{t_{visc}}{t_{max}}$ for $\frac{\dot{M}}{M_E}$ = 0.0001 and 0.0005

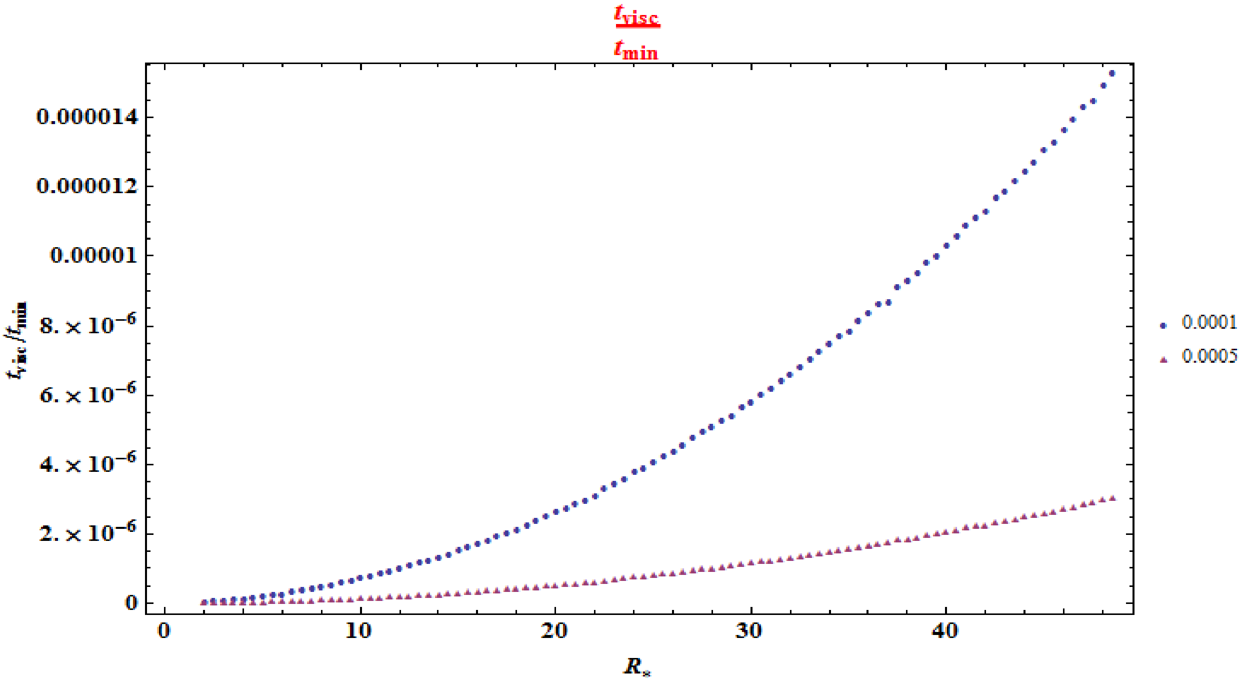

Figure 4.4: $\frac{t_{visc}}{t_{min}}$ for $\frac{\dot{M}}{M_E}$ = 0.0001 and 0.0005

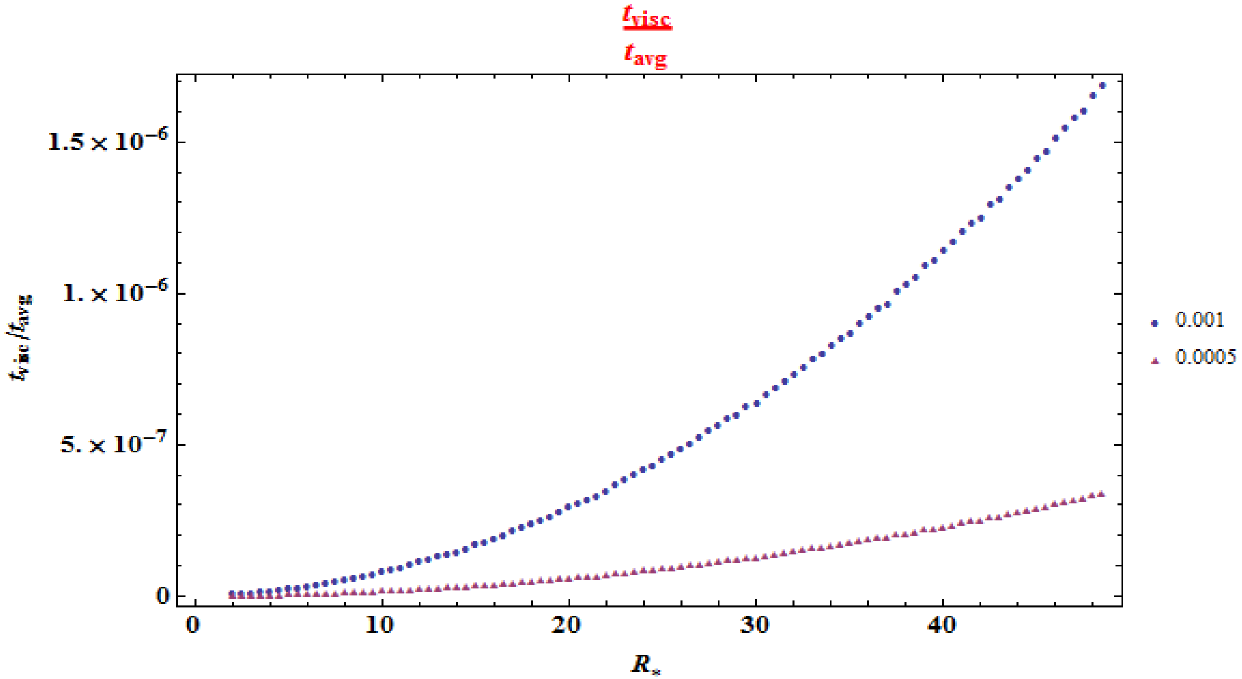

Figure 4.5: $\frac{t_{visc}}{t_{avg}}$ for $\frac{\dot{M}}{M_E} = 0.0001$ and 0.0005

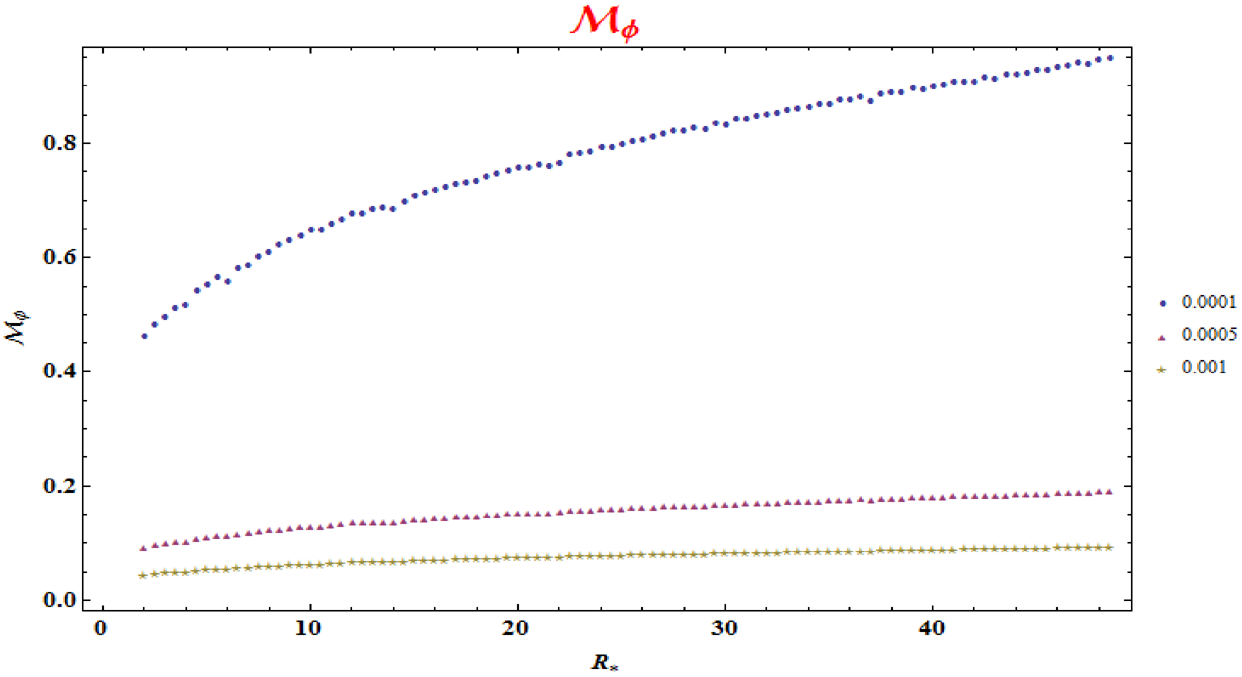

Figure 4.6: $\mathcal{M}_\phi$ for different accretion rates for Kolmogorov process

Chapter 5

Results and Discussion

5.1 Summary

Accretion process is speculated to be related to many transient astrophysical phenomena. We started out with the aim to understand the viscosity mechanism responsible for transport of angular momentum in accretion disks around black holes, to be able to explain some of the observations of X-ray variations from AGNs. We studied two mechanisms, first with ion inertial length as magnetic coherence length. We then looked at the viscosity defined by the radial diffusion of ions across large-scale toroidal magnetic field. We currently have the following results at hand:

- We have an accretion disk model with viscosity defined via transport coefficient of ions in the presence of a large-scale magnetic field with turbulence.

$$\eta_{hyb} = 2.511 \tau_{es} \, v_{rms} \, D_c$$

- The ion temperature is very high (10^{12} K). This also provides us with an upper limit on possible accretion rate:

$$\frac{\dot{M}}{M_E} \leq 0.001$$

- The disk comes out to be puffed up with $\dfrac{H}{R} \sim 10^3$. It is optically thin with high ion density in the inner regions which decreases as we move outwards.

- The viscous timescale is of the order $\sim 10^2$ s or a few hours. It is small in the inner region and increases as we move out into the disk.

One of the major problems this model has is the ion temperature going too high which puts a strict limit on accretion rate. We look at some physical aspects and processes going on in the disk.

5.2 Further work

5.2.1 Two temperature condition and Advection dominated flow

Two temperature disks have been studied by many people after being introduced by Shapiro, Lightman and Eardley [3]. The idea is that the ions and electrons are coupled only by Coulomb collisions, we have assumed that there is no other kind of interactions in the gas. The electrons get enough time to come to an equilibrium temperature and the ions also come to an equilibrium, but both the species do not get enough to reach and equilibrium before they are swept inside the black hole. Also, because of more mass and less susceptibility to radiative losses, ions get heated up more by the viscous dissipation. Ions are generally at a temperature of 10^{12} K and electrons around 10^9 K. The thermal balance equation we considered for our model is [15]:

$$\frac{3}{8\pi}\frac{GM\dot{M}}{R^3 H} f_3 = 3.75 \times 10^{21}\, m_i\, ln\Lambda\, N_i^2 \frac{(T_i - T_e)}{T_e^{3/2}} \tag{5.1}$$

Here, $ln\,\Lambda$ is the Coulomb logarithm. The left-hand side is just viscous heat dissipation and the right-hand side is the thermal balance between ions and electrons, in this case, $T_i \geq T_e$. If we assume other kind of thermal interactions between ions and electrons, the equation will have more terms and will give rise to a different disk structure.

The temperature of electrons is limited by Compton scattering while the ions are heated preferentially by the viscous dissipation. The ions are only assumed to cool down via Coulomb collisions, but there might be other processes taking place.

Advection-dominated flow can take place in systems with optically thin disks and sub-

Eddington accretion rates. That is, the accreting gas is not able to cool down efficiently within accretion time. The dissipated viscous energy is stored in the gas as thermal energy which is not able to radiate away and gets advected into the central object [16].

$$Q^{+} - Q^{-} = f\,\nu\,\rho\,R^{2}\,(\frac{d\Omega}{R})^{2} \tag{5.2}$$

f is the ratio of advected energy to heat generated, it measures the degree to which the flow is advection dominated.

Upper limit on accretion rate is relatively relaxed as opposed to one imposed by the two temperature condition. The form of ion thermal energy balance equation 5.1, would change to accommodate an advective term.

5.2.2 Assumptions

There are two important assumptions in play here:

1. Thermal coupling of ions and electrons.
   We have assumed that there is no other interaction between ions and electrons other than Coulomb interaction, leading to difference in temperatures. In magnetized plasma, it may be that ions and electron interact via other mechanisms and reach equilibrium.

2. Heating of ions.
   Ions being more inertial and less prone to radiative losses have assumed to be the recipient of the dissipated viscous energy. But this might not necessarily be the case as there might be other processes undergoing which might heat up the electrons.

5.2.3 Disk-Jet Connection

The inflow and outflow of matter in an accreting system is intricately related to kind of questions we are trying to answer.

1. Though the exact physical origin of jets from Black hole X-ray binaries (BHXRBs) and AGNs is not known, they can be assumed to be expelled magnetically from the central

engine. This hints towards a significant connection between inner regions of accretion disks and the jet ejection.

2. An important reason we look at the X-ray dips observed to compare our viscous timescales is the speculated mechanism behind this process. X-ray emission is observed in the corona, where it is supposed to originate from upscattering of soft accretion disk photons via Compton scattering, which means the X-ray flux is proportional to the number of electron in the disk. The decrease in electron number results in what we see as a dip in the X-ray spectrum. This decrease may be caused by accreting matter accumulating in the corona over several viscous timescales and eventually collapsing into the central black hole.

3. Chatterjee, et al.[2] show that the optical variations from 3C 120 are strongly correlated with the X-ray variations. This suggests both emissions to originate from the same region. Optical emission can be blackbody radiation from the accretion disk.

4. Further evidence comes from the observation of X-ray and optical spectrum during the dip between October 2006 and April 2007. The optical flux starts to decrease around 40 days before the X-ray dip. An obvious conclusion is a perturbation traveling from the outer edge of accretion disk towards inner or the accretion disk collapsing onto the black hole?(Fig. 5.1 [**?**]

We have established that X-rays dips in the spectrum of 3C 120 can arise due to the collapse of the accretion disk corona over several viscous timescales. However, we are yet to arrive at an understanding of the connection between the X-ray dips and the ejection of blobs in the episodic jets as shown by the correlations in Chatterjee, et. al.

We will be studying observations from more system, preferably with sub-Eddington accretion rates and compare the viscous timescales. We need to answer questions like, Is the coronal plasma which collapses into the central black hole redirected into the jet? If so, is it possible to come up with an integrated model that can explain the timescale over which these jet are ejected as well as this emptying out of the coronal plasma?

[2]

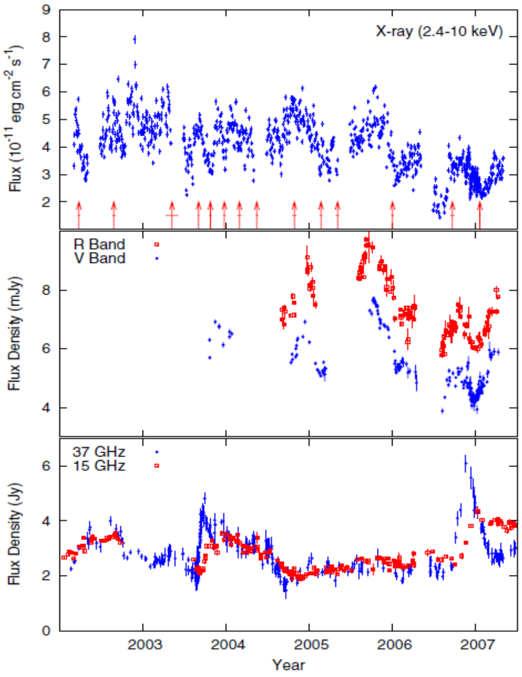

Figure 6. Variation of X-ray flux, optical flux density, and radio flux density of 3C 120 from 2002 to 2007. In the top panel, the arrows show the times of superluminal ejections and the line segments perpendicular to the arrows indicate the uncertainties in the times.

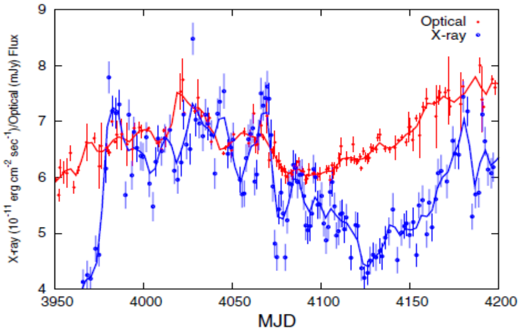

Figure 7. Points represent the X-ray and optical light curves between MJD 3950 and 4200 (2006 October and 2007 April) when the time sampling was dense during a minimum in the light curves. The curves represent the same data smoothed with a Gaussian function with a 3 day FWHM smoothing time.

Figure 5.1: Observation of X-ray, Radio and Optical flux from 3C 120.

Bibliography

[1] N. I. Shakura and R. A. Sunyaev. Black holes in binary systems. Observational appearance. *Astronomy and Astrophysics*, 24:337–355, 1973.

[2] Ritaban Chatterjee, Alan P. Marscher, Svetlana G. Jorstad, Alice R. Olmstead, Ian M. McHardy, Margo F. Aller, Hugh D. Aller, Anne Lähteenmäki, Merja Tornikoski, Talvikki Hovatta, Kevin Marshall, H. Richard Miller, Wesley T. Ryle, Benjamin Chicka, A. J. Benker, Mark C. Bottorff, David Brokofsky, Jeffrey S. Campbell, Taylor S. Chonis, C. Martin Gaskell, Evelina R. Gaynullina, Konstantin N. Grankin, Cecelia H. Hedrick, Mansur A. Ibrahimov, Elizabeth S. Klimek, Amanda K. Kruse, Shoji Masatoshi, Thomas R. Miller, Hong-Jian Pan, Eric A. Petersen, Bradley W. Peterson, Zhiqiang Shen, Dmitriy V. Strel'nikov, Jun Tao, Aaron E. Watkins, and Kathleen Wheeler. DiskJet Connection in the Radio Galaxy 3C 120. *The Astrophysical Journal*, 704(2):1689–1703, 2009.

[3] S L Shapiro, A P Lightman, and D M Eardley. A two-temperature accretion disk model for Cygnus X-1 - Structure and spectrum. *The Astrophysical Journal*, 204:187, 1976.

[4] J. a. Eilek and M. Kafatos. The high energy spectrum of hot accretion disks. *AIP Conference Proceedings*, 101(May 2015):353–353, 1983.

[5] J. a. Eilek. Pair production and gamma-ray luminosities in hot accretion disks. *The Astrophysical Journal*, 236, 1980.

[6] Prasad Subramanian, Peter A. Becker, and Menas Kafatos. Ion Viscosity Mediated by Tangled Magnetic Fields: an Application to Black Hole Accretion Disks. *The Astrophysical Journal*, 469, 1996.

[7] Prasad Subramanian, Alejandro Lara, and Andrea Borgazzi. Can solar wind viscous drag account for coronal mass ejection deceleration? *Geophysical Research Letters*, 39, 2012.

[8] Nishtha Sachdeva, Prasad Subramanian, Robin Colaninno, and Angelos Vourlidas. CME propagation: Where does solar wind drag take over? pages 1–28, 2015.

[9] J Candia and E Roulet. Diffusion and drift of cosmic rays in highly turbulent magnetic fields. *Journal of Cosmology and Astroparticle Physics*, 10(04):7, 2004.

[10] Prasad Subramanian, Peter A Becker, and Menas Kafatos. Using transport coefficients of cosmic rays in turbulent magnetic fields to determine hybrid viscosity in hot accretion disks around AGN. In *Internation Cosmic Ray Conference, Pune*, pages 359–362, 2005.

[11] N. I. Shakura and R. A. Sunyaev. A theory of the instability of disk accretion on to black holes and the variability of binary X-ray sources, galactic nuclei and quasars. *Monthly Notices of the Royal Astronomical Society*, 175(3):613–632, 1976.

[12] T. Piran. The role of viscosity and cooling mechanisms in the stability of accretion disks. *The Astrophysical Journal*, 221:652, 1978.

[13] Alan P. Lightman and Douglas M. Eardley. Black holes in binary systems: Instability of disk accretion. *Astrophys. J., Lett*, 187(1), 1974.

[14] Juhan Frank, Andrew King, and Derek Raine. *Accretion power in Astrophysics.* Cambridge University Press, 2002.

[15] Prasad Subramanian. *No Title.* PhD thesis, George Mason University, 1997.

[16] Ramesh Narayan, Rohan Mahadevan, and Eliot Quataert. Advection-Dominated Accretion around Black Holes. *Arxiv preprint arXiv*, (1988):36, 1998.